SLAC-PUB-5741
SCIPP-92-07
SU-ITP-92-7
February 15, 2001
(T/AS)

TOWARDS THE THEORY OF THE ELECTROWEAK PHASE TRANSITION*

Michael Dine and Robert G. Leigh
Santa Cruz Institute for Particle Physics,
University of California, Santa Cruz, CA 95064

Patrick Huet
Stanford Linear Accelerator Center
Stanford University, Stanford, CA 94309

Andrei Linde †
Department of Physics, Stanford University, Stanford, CA 94305

Dmitri Linde
Gunn High School, Palo Alto, CA 94305

Submitted for Publication to Physical Review D

*Research supported by the Department of Energy under grants 7-443256-22411-3 and DE-AC03-76SF00515, and by the National Science Foundation grant PHY-8612280.
E-mail: LINDE@PHYSICS.STANFORD.EDU; DINE, HUET, LEIGH@SLACVM
†On leave from: Lebedev Physical Institute, Moscow.

ABSTRACT

We investigate various problems related to the theory of the electroweak phase transition. This includes determination of the nature of the phase transition, discussion of the possible role of the higher order radiative corrections and the theory of the formation and evolution of bubbles of the new phase. We show, in particular, that no dangerous linear terms in the scalar field ϕ appear in the expression for the effective potential. We have found, that for the Higgs boson mass smaller than the masses of W and Z bosons, the phase transition is of the first order. However, its strength is approximately 2/3 times less than what follows from the one-loop approximation.

The phase transition occurs due to production and expansion of critical bubbles. Subcritical bubbles may be important only if the phase transition is very weakly first order. A general analytic expression for the probability of the bubble formation is obtained, which may be used for study of tunneling in a wide class of theories.

The bubble wall velocity depends on many factors, including the ratio of the mean free path of the particles to the thickness of the wall. Thin walls in the electroweak theory have a nonrelativistic velocity, whereas thick walls may be relativistic.

Decrease of the cubic term by the factor 2/3 rules out baryogenesis in the minimal version of the electroweak theory. Even though we concentrate in this paper on the phase transition in this theory, most of our results can be applied to more general models as well, where baryogenesis is possible.

1 Introduction

Twenty years ago David Kirzhnits discovered that the symmetry between weak and electromagnetic interactions should be restored at the very early stages of the evolution of the universe [1]. Symmetry breaking between weak and electromagnetic interactions occurs when the universe cools down to a critical temperature $T_c \sim 10^2$ GeV. His results were confirmed by an investigation performed in 1974 by Weinberg, Dolan and Jackiw and by Kirzhnits and Linde [2], and soon the theory of the electroweak phase transition became one of the well established ingredients of modern cosmology. Surprisingly enough, a complete theory of this phase transition is still lacking.

In the first papers on this problem it was assumed that the phase transition is of the second order [1, 2]. Later Kirzhnits and Linde showed [3] that in the gauge theories with many particles, and especially with particles which are much more heavy than the Higgs boson ϕ, one should take into account corrections to the high temperature approximation used in [1, 2]. These corrections lead to the occurrence of cubic terms $\sim g^3\phi^3 T$ in the expression for the effective potential $V(\phi, T)$. As a result, at some temperature, V acquires an extra minimum, and the phase transition is first order [3]. Such phase transitions occur through the formation and subsequent expansion of bubbles of the scalar field ϕ inside the symmetric phase $\phi = 0$. A further investigation of this question has shown that the phase transitions in grand unified theories are always strongly first order [4]. This realization, as well as the mechanism of reheating of the universe during the decay of the supercooled vacuum state suggested in [3, 5], played an important role in the development of the first versions of the inflationary universe scenario [6]. (For a review of the theory of phase transitions and inflationary cosmology see Ref. [7].)

For a long time it did not seem likely that the electroweak phase transition could have any dramatic consequences, unless the Higgs boson is exceptionally light. Even though the possibility of a strong baryon number violation during the electroweak phase transition was pointed out fifteen years ago by Linde [8] and by Dimopoulos and Susskind [9], only after the groundbreaking paper by Kuzmin, Rubakov and Shaposhnikov [10] was it realized that such processes do actually occur and may erase all previously generated baryon asymmetry of the universe.

Recently, the possibility that electroweak interactions may not only erase but also produce the cosmic baryon asymmetry has led to renewed interest in the electroweak phase transition. A number of scenarios have been proposed for generating the asymmetry [11] – [18]. All of them require that the phase transition should be strongly first order since otherwise the baryon asymmetry generated during the phase transition subsequently disappears. In all of these scenarios the asymmetry is produced near the walls of the bubbles of the scalar field ϕ. Thus, an understanding of the nature of the phase transition in the electroweak theory and investigation of the structure of the bubbles produced during the phase transition are of some importance. For this purpose one should make a much more thorough analysis of the electroweak phase transition than the analysis which is necessary for an approximate calculation of the critical temperature.

Unfortunately, despite the fact that one is dealing with a weakly coupled theory, many aspects of the phase transition are surprisingly complicated. Indeed, the literature contains contradictory claims and statements on almost every important question. In this paper, we will attempt to resolve a number of these questions, or at least to delineate the issues which are crucial to a complete analysis. We will confine our attention to weakly coupled theories, not because strongly coupled theories (e.g. technicolour theories) are not of interest, but simply because we will find these problems quite difficult even in theories with explicit Higgs particles. Even more specifically, we will discuss the simplest version of the electroweak theory containing only one Higgs boson. We doubt that the baryon asymmetry can be generated in this simple model; in fact, we will find some new evidence against it. However, this model will help us to illustrate various possibilities which may be realized in more complicated theories.

The first problem to be studied is whether the phase transition is first order, and precisely how strongly first order it may be. One clear requirement arises if no net $B-L$ is produced at the transition (in the model of [16] a net $B-L$ is produced). In this circumstance, as first stressed in [11], the rate of baryon number violating transitions after the phase transition is completed must be smaller than the expansion rate. In practice, this means that the ratio of the Higgs field ϕ inside the bubble to the temperature T cannot be smaller than one, in order that the sphaleron energy not be too small.

This condition was used in [11, 19] to impose a strong constraint on the Higgs mass in the minimal version of the electroweak theory, $m_H \lesssim 42$ GeV. This, of course, already contradicts the present experimental limits $m_H \gtrsim 57$ GeV [20]. However, more careful consideration of various theoretical uncertainties indicated that the constraint might be somewhat weaker, permitting m_H up to 55 GeV, or possibly higher [21]. In any case, successful baryogenesis almost certainly requires some extension of the standard model, possibly including more scalar fields. In multi-Higgs models [19, 14], the limits are substantially weaker. Indeed, Anderson and Hall [22] have noted that simply adding a scalar singlet to the model significantly weakens the constraint.

Before one can discuss details of the process of baryogenesis, it is necessary to check that the results of our investigation of the phase transition are reliable. This is not a trivial issue even in the minimal electroweak theory. Indeed, as stressed in Refs. [3, 5], each new order of perturbation theory at finite temperature may bring a new factor of $g^2T/m \sim gT/\phi$ for the theories with gauge boson masses $m \sim g\phi$. This means that the results of the one loop calculations may become unreliable at $\phi \lesssim gT$. A rather unexpected (and often overlooked) consequence of this observation is that we cannot even say in an absolutely reliable way that symmetry at high temperatures is completely restored; one may say only that the strength of the symmetry breaking is limited by the constraint $\phi < gT$, $m < g^2T$ [7]. In theories with $g \ll 1$ this result is quite informative. However, gauge coupling constants in the electroweak theory are not *much* smaller than one. Therefore, the reliability of our results concerning the region $\phi \lesssim T$ deserves a detailed investigation.

This issue became more urgent with the recent claim by Brahm and Hsu that higher order corrections lead to the appearance of a term in the effective potential $\sim -g^3\phi T^3$ [23]. This term is linear in ϕ; it is very large at small ϕ, and it removes the local minimum of $V(\phi, T)$ created by the cubic term $\sim -g^3\phi^3 T$. As a result, the phase transition ceases to be first order. In fact, the phase transition ceases to be a phase transition, since the scalar field does not vanish at any temperature. At large temperature the scalar field remains smaller than gT, which means that this result is not in direct contradiction with our earlier conclusions. But still, the result of Ref. [23] seems somewhat surprising.

The importance of understanding these issues has been highlighted even more dramatically by the recent work of Shaposhnikov [24]. He has also found a linear term in the effective potential, but with an opposite sign! Shaposhnikov concludes that the phase transition is much more strongly first order than expected. He argues that baryogenesis in the minimal electroweak model is possible despite the problems with the CP violation and obtains an improved constraint on the Higgs boson mass, $m_H \lesssim 64$ GeV, which is quite consistent with the experimental constraints. Thus, without a proper study of the higher order corrections to the effective potential, one may be unable to make any conclusions concerning the possibility of baryogenesis in the standard model.

The authors of Refs. [23, 24] obtained linear terms by simply substituting the effective masses found at one loop back into the one loop calculation of $V(\phi, T)$. Such a procedure is generally reliable when calculating Green's functions, or tadpoles corresponding to $\frac{dV}{d\phi}(\phi, T)$. However, it leads to combinatoric errors when calculating the free energy. Our investigation of this problem shows that if one is careful with counting of Feynman diagrams and with gauge invariance, neither positive nor negative linear terms $\sim g^3\phi T^3$ appear in the effective potential [25].

Moreover, we will argue that, despite all uncertainties with higher order corrections, the expectation value of the scalar field ϕ actually disappears, $\phi = 0$, at a temperature higher than some critical temperature T_o. (Note, that this would be impossible in the presence of linear terms of either sign.)

However, high order corrections do lead to a definite and significant modification of the one-loop results. Namely, they lead to a decrease of the cubic term $g^3\phi^3 T$ by a factor 2/3. This effect decreases the ratio ϕ/T at the point of the phase transition by approximately the same factor 2/3. This makes baryogenesis virtually impossible in the context of the minimal standard model with $m_H > 57$ GeV.

Assuming that one knows the shape of the effective potential at small ϕ, one should still work hard to determine the ratio ϕ/T at the point of the phase transition. One needs to know at what temperature the transition actually occurs, and some details of *how* it occurs. At very high temperatures the effective potential of the Higgs field, $V(\phi, T)$, has a unique minimum

at the symmetric point $\phi = 0$. As the temperature is lowered, a second minimum appears. At a critical value T_c, this second minimum becomes degenerate with the first one. However, the phase transition actually occurs at a somewhat lower temperature, due to the formation of bubbles of true vacuum which grow and fill the universe. The usual way to study bubble formation is to use the euclidean approach to tunneling at a finite temperature [27]. One should find high-temperature solutions, which describe the so-called critical bubbles. Then one should calculate their action, which leads to an exponential suppression of the probability of bubble formation. Typically, these calculations are rather complicated, and analytic results can only be obtained in a few cases. One of these is the thin wall approximation, which is valid (as in the case of transitions at zero temperature) if the difference in depth of the two minima of $V(\phi, T)$ is much smaller than the height of the barrier between them. In this case the radius of the bubble at the moment of its formation is much larger than the size of the bubble wall, and the properties of the bubble can be obtained very easily. Recently Anderson and Hall performed a thorough analytic study of the phase transition in the electroweak theory in one loop approximation [22]. Their results for the one loop effective potential $V(\phi, T)$ completely agree with the results of our investigation [21]. However, in their study of the bubble formation they assumed that the thin-wall approximation is applicable. As we will see, for the Higgs boson masses in the range of interest, $m_H < m_W$, this is not the case even if one takes into account modification of the cubic terms by higher order corrections. Fortunately, we were able to obtain a simple analytic expression which gives the value of the euclidean action for theories with an effective potentials of a rather general type, $V(\phi, T) = a\phi^2 - b\phi^3 + c\phi^4$. We hope that this result will be useful for a future investigation of bubble formation in a wide class of gauge theories with spontaneous symmetry breaking.

On the other hand, validity of the standard assumption that the phase transition occurs due to formation of critical bubbles should be verified as well. Kolb and Gleiser [28] and, more recently, Tetradis [29] have argued that the phase transition may occur by a different mechanism, the formation of small (subcritical) bubbles. If this is the case, the transition is completed earlier and by a different mechanism than in the conventional picture. While this idea is very interesting, we will argue that it is only relevant in cases where the transition is very weakly first order and the euclidean action cor-

responding to critical bubbles is not much larger than one. This is not the case for the strongly first order phase transitions, where the relevant value of the euclidean action at the moment of the transition is $S \sim 130 - 140$.

Determination of the baryon asymmetry produced at the phase transition requires knowledge not only of how bubbles are produced, but also of how they evolve. Because the expansion of the universe is so slow at this time, a typical bubble grows to a macroscopic size before colliding with other bubbles. In the first scenarios proposed for the formation of the asymmetry, baryon number was produced in the bubble wall [11] – [17]. This mechanism, at best, is not terribly efficient, because the baryon number violating processes turn off rapidly as the scalar field expectation value turns on. The resulting asymmetry is sensitive to the speed and thickness of the bubble.[1] The most effective scenarios for electroweak baryogenesis have the baryons produced in front of the wall, in the symmetric phase [18]. In this picture, scattering, for example, of top quarks from the bubble wall leads to an asymmetry in left vs. right-handed top quarks in a region near the wall. This asymmetry, resulting from an asymmetry between reflection and transmission of different quark helicities at the wall, biases the rate of baryon number violation in the region in front of the wall; the resulting value of n_b/n_γ can be as large as 10^{-5}. However, the authors of Ref. [18] assumed that the wall was rather thin, with a thickness of order T^{-1}. For thicker walls, the asymmetry goes rapidly to zero. This can easily be understood. In order to have an asymmetry in reflection coefficients, the top quarks must have enough energy to pass through the wall. For $m_t \sim 120$ GeV, this means typically the energy must be greater than about $T/2$. If the wall is very thick compared to this scale, the motion of the top quarks is to a good approximation semiclassical, and the reflection coefficient is exponentially suppressed. The analyses of other authors also exhibit sensitivity to the wall shape and velocity.

Clearly, then, it is important to understand how the bubble propagates after its initial formation. In this paper we will consider some aspects of this problem. A complete description of the wall evolution is rather complicated. We will see, however, that in certain limits it is not too difficult to determine how the velocity and thickness of the wall depend on the underlying model

[1] The extent of this suppression and the precise form of this dependence is still a subject of debate.

parameters. In this analysis, it is crucial to recall that in addition to the various microscopic parameters, there is another parameter of great importance: the expansion rate of the universe. Imagine a world with arbitrarily small value of Newton's constant. In such a world, the phase transition occurs at a temperature arbitrarily close to T_c and the pressure difference on the two sides of the wall is arbitrarily small. Thus, in this limit one expects that the wall will move arbitrarily slowly, and a systematic expansion of the relevant physical quantities in powers of the wall velocity should be possible. Since in the real world, the expansion rate of the universe is indeed quite small at T_c, it seems plausible that the real velocity of the wall should be small, and that the expansion in powers of velocity should be a fair approximation. Even within the framework of this small velocity approximation, we will content ourselves with a quite crude picture for the processes which damp the wall's motion. Within this framework, we will find that for plausible values of Higgs masses, the wall velocity is indeed small, varying from $v \sim .01$ to $v \sim 0.3$; at the same time the wall will typically have a thickness of order 10's of T^{-1}'s.

There have been a number of attempts in the past to compute the wall parameters, including efforts by some of the present authors. In Ref. [27] a simple formula for the wall velocity was given, based on a semiclassical picture in which one species of particles gains a large mass $M \gg T$ as it passes through the wall. Balancing the force on the wall due to these particles with the pressure difference between the two phases gives a relation of the form

$$v = \frac{\Delta p}{\Delta \rho} \ , \tag{1}$$

where p is the pressure and ρ is the internal energy. We will see that an expression of this form holds only if the mean free paths of the particles are large compared to the thickness of the wall, and that this condition is not likely to hold for the electroweak transition. We will argue that the actual wall velocity is somewhat larger than would be expected from this formula.

In Ref. [15], a different approach was adopted. Assuming the temperature and velocity are constant across the wall, momentum and energy conservation give an expression for the velocity of the form

$$v^2 \sim \frac{\Delta p}{\Delta \rho} \ . \tag{2}$$

As we will see in the present investigation, however, one cannot neglect the change in temperature and velocity of the gas as it passes the wall. For relativistic gases, one always obtains expressions linear in the velocity.

More recently, Turok has argued [30] that these types of analyses are incorrect. He suggests that reflection of particles from the wall does not slow the wall at all. Indeed, he argues that the only way in which the wall can dissipate energy is through rather complicated particle production processes, suppressed by several powers of coupling constant. As a result, even if the phase transition is very weakly first order, the bubble wall becomes ultrarelativistic. To buttress his case, Turok shows that if the gas is everywhere in thermal equilibrium (corresponding to the local value of the scalar field) then the force on the wall is independent of the velocity. This is indeed correct. However, all of the effects we find arise because of small, velocity-dependent departures from equilibrium.[2]

To a large extent, our analysis will be an extension of the semiclassical reasoning of Ref. [27]. We begin by pointing out that there is an important assumption made more or less explicitly in all of these analyses: that by the time the wall has grown to a macroscopic size, it has achieved a steady state. If this is the case, the problem can be analyzed in the rest frame of the wall, where the scalar field and the particle distributions are independent of time. We describe a simple situation (due to L. Susskind) where this is not the case, and which we refer to as the 'snowplow.' In this situation, there is a steady pileup of particles near the wall. While we do not expect that precisely this snowplow phenomenon occurs in the cases of interest, it makes clear that there are additional, potentially important effects which must be taken into account and which are left out of existing treatments. We then consider there three limiting situations. In the first of these, a typical particle does not scatter off of other particles of the gas as it passes through the wall. This 'thin wall' case is that for which (a modification of) eq. (1) is valid, and tends to give a very small value for the wall velocity. In the second case, the wall is thick compared both to typical mean free paths for elastic scattering and for scatterings which change the numbers of different

[2]Turok and McLerran have recently informed us that they have reconsidered the argument of [30] and have argued that there are additional sources of damping, including scattering of particles from the wall.

particle types. In this case, the gas is nearly in equilibrium everywhere. The velocity is larger than in the thin wall case by a factor of order $\sqrt{\frac{\delta}{\ell}}$, where ℓ is some typical mean free path and δ is the wall thickness. In the third situation, the wall is thick compared to typical mean free paths for elastic scattering, but not for scatterings which change particle number. Thus, one has some approximate kinetic equilibrium locally, but particle numbers are not equilibrated in the wall. This is the situation which appears to have greatest relevance to the electroweak transition. Here, phenomena similar to the snowplow effect occur, and there is an enhancement of the density of tops, W's and Z's in the wall. This tends to reduce the wall velocity, giving a result intermediate between the thin and thick wall cases.

The plan of the paper is the following. In Section 2 we will describe the phase transition in the electroweak theory in one loop approximation. In Section 3 we will consider the theory of bubble formation during the phase transition. Section 4 will contain a discussion of role of the higher order corrections. In Section 5 we will deal with the issue of subcritical bubbles. Finally, in Section 6, the bubble wall propagation will be considered. Details of relevant calculations will be contained in the Appendix.

2 The Phase Transition

Let us consider the form of the effective potential at finite temperature. Contributions of particles of a mass m to $V(\phi, T)$ are proportional to $m^2 T^2$, $m^3 T$ and $m^4 \ln(m/T)$. We will assume that the Higgs boson mass is smaller than the masses of W and Z bosons and the top quark, $m_H < m_W, m_Z, m_t$. Therefore we will neglect the Higgs boson contribution to $V(\phi, T)$.

The zero temperature potential, taking into account one-loop corrections, is given by [7]

$$V_0 = -\frac{\mu^2}{2}\phi^2 + \frac{\lambda}{4}\phi^4 + 2Bv_o^2\phi^2 - \frac{3}{2}B\phi^4 + B\phi^4 \ln(\frac{\phi^2}{v_o^2}) \ . \tag{3}$$

Here

$$B = \frac{3}{64\pi^2 v_o^4}(2m_W^4 + m_Z^4 - 4m_t^4) \ , \tag{4}$$

$v_o = 246$ GeV is the value of the scalar field at the minimum of V_0, $\lambda = \mu^2/v_o^2$, $m_H^2 = 2\mu^2$. Note that these relations between λ, μ, v_o and the Higgs boson mass m_H, which are true at the classical level, are satisfied even with an account taken of the one-loop corrections. This is an advantage of the normalization conditions used in [7]. An expression used in [22] is equivalent to this expression up to an obvious change of variables.

At a finite temperature, one should add to this expression the term

$$V_T = \frac{T^4}{2\pi^2}\Big(6I_-(y_W) + 3I_-(y_Z) - 6I_+(y_t)\Big) \ , \tag{5}$$

where $y_i = M_i\phi/v_oT$, and

$$I_\mp(y) = \pm\int_0^\infty dx\ x^2 \ln(1 \mp e^{-\sqrt{x^2+y^2}}) \ . \tag{6}$$

The results of our work are based on numerical calculation of these integrals, without making any specific approximations [21]. However, in the large temperature limit it is sufficient to use an approximate expression for $V(\phi, T)$ [1, 22],

$$V(\phi, T) = D(T^2 - T_o^2)\phi^2 - ET\phi^3 + \frac{\lambda_T}{4}\phi^4 \ . \tag{7}$$

Here

$$D = \frac{1}{8v_o^2}(2m_W^2 + m_Z^2 + 2m_t^2) \ , \tag{8}$$

$$E = \frac{1}{4\pi v_o^3}(2m_W^3 + m_Z^3) \sim 10^{-2} \ , \tag{9}$$

$$T_o^2 = \frac{1}{2D}(\mu^2 - 4Bv_o^2) = \frac{1}{4D}(m_H^2 - 8Bv_o^2) \ , \tag{10}$$

$$\lambda_T = \lambda - \frac{3}{16\pi^2 v_o^4}\left(2m_W^4 \ln\frac{m_W^2}{a_B T^2} + m_Z^4 \ln\frac{m_Z^2}{a_B T^2} - 4m_t^4 \ln\frac{m_t^2}{a_F T^2}\right) \ , \tag{11}$$

where $\ln a_B = 2\ln 4\pi - 2\gamma \simeq 3.91$, $\ln a_F = 2\ln\pi - 2\gamma \simeq 1.14$.

To avoid misunderstandings, we should note again that due to our choice of more convenient renormalization conditions, the form of some of our equations is slightly different from the form of expressions used in [22]. In particular, instead of large coefficients c_B and c_F in the equation for λ_T in [22], we

have smaller constants a_B and a_F. However, all physical results obtained by our equations coincide with the one-loop results of Refs. [21, 22].

The behavior of $V(\phi, T)$ is reviewed in Refs. [7, 31]. It will be useful for our future discussion to identify several 'critical points' in the evolution of $V(\phi, T)$.

At very high temperatures the only minimum of $V(\phi, T)$ is at $\phi = 0$. A second minimum appears at $T = T_1$, where

$$T_1^2 = \frac{T_o^2}{1 - 9E^2/8\lambda_{T_1} D} \ . \tag{12}$$

The value of the field ϕ in this minimum at $T = T_1$ is equal to

$$\phi_1 = \frac{3ET_1}{2\lambda_{T_1}} \ . \tag{13}$$

The values of $V(\phi, T)$ in the two minima become equal to each other at the temperature T_c, where

$$T_c^2 = \frac{T_o^2}{1 - E^2/\lambda_{T_c} D} \ . \tag{14}$$

At that moment the field ϕ in the second minimum becomes equal to

$$\phi_c = \frac{2ET_c}{\lambda_{T_c}} \ . \tag{15}$$

The minimum of $V(\phi, T)$ at $\phi = 0$ disappears at the temperature T_o, when the field ϕ in the second minimum becomes equal to

$$\phi_o = \frac{3ET_o}{\lambda_{T_o}} \ . \tag{16}$$

The results of a numerical investigation of $V(\phi, T)$ for a particular case, $m_H = 50$ GeV and $m_t = 120$ GeV, are shown in Fig. 1.

3 Bubble Formation

In the previous section we noted that the two minima of $V(\phi, T)$ become of the same depth at the temperature T_c, eq. (14). However, tunneling with

formation of bubbles of the field ϕ corresponding to the second minimum starts somewhat later, and it goes sufficiently fast to fill the whole universe with the bubbles of the new phase only at some lower temperature T when the corresponding euclidean action suppressing the tunneling becomes less than 130 – 140 [13, 21, 22]. Some small uncertainty in this number is related to the speed with which bubble walls move after being formed (see the next section) and to the exact value of the critical temperature, which is very sensitive to the top quark mass and to the value of the cubic term. In this paper (see also [21]) we performed a numerical study of the probability of tunneling. Before reporting our results, we will remind the reader of some basic concepts of the theory of tunneling at a finite temperature.

In the euclidean approach to tunneling (at zero temperature) [34], the probability of bubble formation in quantum field theory is proportional to $\exp(-S_4)$, where S_4 is the four-dimensional Euclidean action corresponding to the tunneling trajectory. In other words, S_4 is the instanton action, where the instanton is the solution of the euclidean field equations describing tunneling. A generalization of this method for tunneling at a very high temperature [27] gives the probability of tunneling per unit time per unit volume

$$P \sim A(T) \cdot \exp(-\frac{S_3}{T}) \ . \tag{17}$$

Here $A(T)$ is some subexponential factor roughly of order T^4; S_3 is a three-dimensional instanton action. It has the same meaning (and value) as the fluctuation of the free energy $F = V(\phi(\vec{x}), T)$ which is necessary for bubble formation. To find S_3, one should first find an $O(3)$-symmetric solution, $\phi(r)$, of the equation

$$\frac{d^2\phi}{dr^2} + \frac{2}{r}\,\frac{d\phi}{dr} = V'(\phi) \ , \tag{18}$$

with the boundary conditions $\phi(r = \infty) = 0$ and $d\phi/dr|_{r=0} = 0$. Here $r = \sqrt{x_i^2}$; the x_i are the euclidean coordinates, i = 1,2,3. Then one should calculate the corresponding action

$$S_3 = 4\pi \int_0^\infty r^2 \ dr[\frac{1}{2}\left(\frac{d\phi}{dr}\right)^2 + V(\phi(r), T)] \ . \tag{19}$$

Usually it is impossible to find an exact solution of eq. (18) and to

calculate S_3 without the help of a computer. A few exceptions to this rule are given in Refs. [7, 27]. One of these exceptional cases is realized if the effective potential has two almost degenerate minima, such that the difference ε between the values of $V(\phi, T)$ at these minima is much smaller than the energy barrier between them. In such a case the thickness of the bubble wall at the moment of its formation is much smaller than the radius of the bubble, and the action S_3 can be calculated exactly as a function of the bubble radius r, the energy difference ΔV and the bubble wall surface energy S_1:

$$S_3 = -\frac{4\pi}{3} r^3 \Delta V + 4\pi r^2 S_1 \ , \tag{20}$$

where

$$S_1 = \int_0^\infty d\phi \sqrt{2V(\phi, T)} \ . \tag{21}$$

The radius of the critical bubble r can be found by finding an extremum of $S_3(r)$. However, one must be very careful when using these results. Indeed, as can be easily checked, this extremum is not a *minimum* of the action, it is a *maximum*. (This just corresponds to the fact that critical bubbles are unstable and either expand or contract). Similarly, the action corresponding to the true solution of eq. (18) will be higher than the action of any approximate solution. As a result, one can strongly overestimate the tunneling probability by calculating it outside the limit of validity of the thin wall approximation. For example, in Ref. [22] the phase transition in the electroweak theory with $m_H \sim 50$ GeV was studied and it was found that it happens very soon after the temperature approaches T_c, occurring due to formation of bubbles with thin walls. According to [22], this happens at $\epsilon = 1/6$, where $\epsilon = \frac{T_c^2 - T^2}{T_c^2 - T_o^2}$. However, the authors did not check the validity of the thin wall approximation in this case. Whereas our one-loop results for the effective potential $V(\phi, T)$ are in complete agreement with the results of Ref. [22], our conclusion concerning the bubble formation is somewhat different. As we have already mentioned, the phase transition in the electroweak theory is completed when the ratio S_3/T becomes about 130 – 140. Our calculations show that this happens at $\epsilon \sim 1/4$. In Fig. 1 we plot the shape of the effective potential and in Fig. 2 the shape of the solution of eq. (18) corresponding to $S_3/T \sim 140$ for $m_H = 50$ GeV and $m_t = 120$ GeV. (The results for tunneling and for the ratio ϕ/T prove to be not very sensitive to the mass of the top quark in the interval $100 \text{ GeV} \lesssim m_t \lesssim 150$

GeV.) The effective potential $V(\phi, T)$ at $\epsilon = 1/6$ looks very similar, but the value of S_3/T in this case is about 300, which is 3 times larger than the result obtained in [22] in the thin wall approximation. It is clear from these figures and the results of numerical calculations of S_3/T that the thin wall approximation is far from being applicable for the investigation of the phase transition in the electroweak theory, unless the phase transition is weakly first order. However, the last case is not particularly interesting from the point of view of baryon asymmetry generation.

We must note, that the numerical results obtained above are modified when one takes into account higher order corrections to the effective potential. As we will show in the next section, these corrections change the numerical value of the coefficient E in the cubic term in (7). The final numerical results of our study of the probability of tunneling will be contained, therefore, in the next section. Here we just wanted to show the difference between the results of the numerical investigation of tunneling and the results obtained in the thin wall approximation. This difference remains large after the modification of the coefficient E.

We would now like to obtain an analytic estimate of the probability of tunneling in the electroweak theory, which can be used for any particular numerical values of constants D, E and λ_T. As shown in Ref. [22], eq. (7) in most interesting cases approximates $V(\phi, T)$ with an accuracy of a few percent. This by itself does not help very much if one must study tunneling anew for each new set of the constants. However, it proves possible to reduce this study to the calculation of one function $f(\alpha)$, where α is some ratio of constants D, E and λ_T. In what follows we will calculate this function for a wide range of values of α. This will make it possible to investigate tunneling in the electroweak theory without any further use of computers.

First of all, let us represent the effective Lagrangian $L(\phi, T)$ near the point of the phase transition in the following form:

$$L(\phi, T) = \frac{1}{2}(\partial_\mu \phi)^2 - \frac{M^2(T)}{2}\phi^2 + ET\phi^3 - \frac{\lambda_o}{4}\phi^4 \ . \qquad (22)$$

Here $M^2(T) = 2D(T^2 - T_o^2)$ is the effective mass squared of the field ϕ near the point $\phi = 0$, λ_t is the value of the effective coupling constant λ_T near the point of the phase transition (i.e. at $T \sim T_t$, where T_t is the temperature

at the moment of tunneling). With a very good accuracy, the constants $\lambda_t, \lambda_{T_1}, \lambda_{T_c}, \lambda_{T_o}$ are equal to each other.

Defining $\phi = \frac{M^2}{2ET}\Phi$, $x = X/M$, the effective Lagrangian can be written as:

$$L(\Phi, T) = \frac{M^6}{4E^2T^2}\Big[\frac{1}{2}(\partial_\mu\Phi)^2 - \frac{1}{2}\Phi^2 + \frac{1}{2}\Phi^3 - \frac{\alpha}{8}\Phi^4\Big] \ , \tag{23}$$

where

$$\alpha = \frac{\lambda_o M^2}{2E^2T^2} \ . \tag{24}$$

The overall factor $\frac{M^6}{4E^2T^2}$ does not affect the Lagrange equation

$$\frac{d^2\Phi}{dR^2} + \frac{2}{R}\frac{d\Phi}{dR} = \Phi - \frac{3}{2}\Phi^2 + \frac{1}{2}\alpha\Phi^3 \ . \tag{25}$$

Solving this equation and integrating over $d^3X = M^{-3}d^3x$ gives the following expression for the corresponding action:

$$\frac{S_3}{T} = \frac{4.85\,M^3}{E^2\,T^3} \times f(\alpha) \ . \tag{26}$$

The function $f(\alpha)$ is shown in Fig. 3. It is equal [27] to 1 at $\alpha = 0$, and blows up when α approaches 1. In the interval from 0 to 0.95 this function, with an accuracy about 1%, is given by the following simple expression:

$$f(\alpha) = 1 + \frac{\alpha}{4}\Big[1 + \frac{2.4}{1-\alpha} + \frac{0.26}{(1-\alpha)^2}\Big] \ . \tag{27}$$

In the vicinity of the critical temperature T_o, i.e. at $\Delta T \equiv T - T_o \ll T_o$, the action (26) can be written in the following form:

$$\frac{S_3}{T} = \frac{38.8\,D^{3/2}}{E^2} \cdot \Big(\frac{\Delta T}{T}\Big)^{3/2} \times f\Big(\frac{2\,\lambda_o\,D\,\Delta T}{E^2\,T}\Big) \ . \tag{28}$$

Using these results, one can easily get analytical expressions for the tunneling probability in a wide class of theories with spontaneous symmetry breaking, including GUTs and the minimal electroweak theory.

4 Infrared Problems and Reliability of the Perturbation Expansion

In our previous discussion, we have considered only the one loop corrections to the effective potential. In this section we discuss the role of higher order corrections.

Early investigations of the electroweak phase transition [1] did not take into account corrections due to strong interactions, since at that time most physicists did not expect that top quarks would be heavier than W and Z bosons, and thus their contributions were not expected to be terribly important. Given what we now know about the top quark mass, it appears that top quarks give the largest contribution to the parameters D and λ_T in eqs. (8), (11). Thus, it is natural to ask whether strong interaction corrections are likely to be important.

Our preliminary investigation of this question indicates that this is not the case. For example, one of the most important effects would be a change of the Fermi distribution at a finite temperature due to the modification of the quark mass by interactions with gluons. According to [33], quarks at a high temperature acquire a correction to their effective mass squared,

$$\Delta m_t^2(T) = \frac{g_s^2}{6} T^2 \tag{29}$$

with g_s the strong coupling constant.[3] This gives $\Delta m_t^2(T) \sim 0.2\, T^2$ at the temperature of the electroweak phase transition, $T \sim 10^2$ GeV. A similar contribution to the boson mass could lead to important effects (see below). However, due to Fermi statistics, fermion propagators contain terms $[(2n+1)\,\pi\, T]^2$ [7]. As a result, all thermodynamic quantities rather weakly depend on the effective mass squared of the fermions, until this mass becomes comparable with πT.

One should note, of course, that $\Delta m_t^2(T) \sim 0.2\, T^2$ is not a true correction to the top quark mass squared; rather it is a square of the mass gap in the spectrum of fermionic excitations. Therefore a more detailed analysis of

[3] We use $\alpha_s \sim 0.1$ for our estimates.

the higher-loop diagrams involving strong interactions is desirable. Nevertheless, our estimate suggests that the strong interaction effects are actually insignificant for the description of the phase transition. They just lead to a small modification of the critical temperature. More importantly, they do not change cubic terms $\sim g^3\phi^3 T$ in the effective potential and do not induce linear terms $\sim g^3\phi T^3$.

However, higher order corrections in weak interactions at $T \geq T_c$ may be very important. It is well known that, in field theories of massless particles, perturbation theory at finite temperature is subject to severe infrared divergence problems. For small values of the scalar field, the gauge bosons (and near the phase transition, the Higgs boson) are nearly massless; as a result, as was pointed out in the early work on this subject [3, 5], one cannot reliably compute the effective potential for very small ϕ. In this section, we attempt to determine whether the standard one loop calculation of V is indeed reliable in the range of ϕ relevant to our analysis. One might worry, for example, that since the term $-ET\phi^3$ in the effective potential, which leads to the first order phase transition, is important only for rather small ϕ, there might be large corrections changing the order of the phase transition. We will show that indeed the coefficient of the ϕ^3 term is altered to 2/3 of its one loop value. This renders the phase transition, for a given value of the couplings, less first order and can have significant effects on baryogenesis. On the other hand, we will argue that perturbation theory is not in terribly bad shape, and that one can determine the nature of the phase transition with some confidence from low order calculations.

Recently, in a very interesting paper, Brahm and Hsu reach the opposite conclusion [23]. These authors find that at small ϕ, higher order corrections to the scalar field contribution to the effective potential contain a large negative linear term $-g^3\phi T^3$, which eliminates any trace of a first order transition. They argue, moreover, that their calculation is reliable, *i.e.* that all other higher order corrections are under control and do not modify their conclusion.

On the other hand, Shaposhnikov considers higher order corrections to the vector particle contribution to $V(\phi, T)$ and finds a large positive term $+g^3\phi T^3$. He concludes that the phase transition is strongly first order

$(\phi/T > 1)$ even for $m_H \sim 64$ GeV [24].

We will show that neither positive nor negative linear terms appear in the expression for $V(\phi, T)$ if one studies higher order corrections paying particular attention to the correct counting of Feynman diagrams. [25]. We will employ two separate approaches to this problem: a straightforward enumeration of Feynman diagrams, and an effective action analysis valid for a discussion of infrared effects.

We will consider here for simplicity the contribution of the scalar particles and the W bosons only; adding the contribution of Z bosons is trivial. As we have already noted, for questions of infrared behavior, fermions may be ignored. Coulomb gauge, $\vec{\nabla} \cdot \vec{W} = 0$, is particularly convenient for the analysis, though the problem can be analyzed in other gauges as well. In this gauge, the vector field propagator $D_{\mu\nu}$ after symmetry breaking (and after a proper diagonalization) splits into two pieces, the Coulomb piece, D_{00}, and the transverse piece, D_{ij}. For non-zero values of the discrete frequency, $\omega_n = 2\pi n T$, the Coulomb piece mixes with the 'Goldstone' boson. However, for the infrared problems which concern us here, we are only interested in the propagators at zero frequency. For these there is no mixing. One has [3]

$$D_{00}(\omega = 0, \vec{k}) = \frac{1}{\vec{k}^2 + m_W^2(\phi)} \tag{30}$$

and

$$D_{ij}(\omega = 0, \vec{k}) = \frac{1}{\vec{k}^2 + m_W^2(\phi)} P_{ij}(\vec{k}) \ , \tag{31}$$

where $P_{ij} = \delta_{ij} - \frac{k_i k_j}{\vec{k}^2}$. The mass of the vector field W at the classical level is given by $m_W = g v_o/2$. Propagators of the Higgs field ϕ and of the 'Goldstone' field χ in this gauge are given by

$$D_\phi(\vec{k}) = \frac{1}{\vec{k}^2 + m_\phi^2} \ , \tag{32}$$

$$D_\chi(\vec{k}) = \frac{1}{\vec{k}^2} \ . \tag{33}$$

Let us review several ways of obtaining the standard one-loop expression for the cubic term in the effective potential, eq. (7). The most straightforward is to carefully expand eq. (5) for the effective potential in $y_W =$

$\frac{m_W}{v_o T} = \frac{g\phi}{2T}$. Indeed, the contribution of W-bosons to the effective potential at $T > m_W(\phi)$ is given by

$$\begin{aligned} V_W(\phi, T) &= 2 \times 3 \times \Big(-\frac{\pi^2}{90} T^4 + \frac{m_W^2(\phi)}{24} T^2 - \frac{m_W^3(\phi)}{12\pi} T + \cdots \Big) \\ &= 2 \times 3 \times \Big(-\frac{\pi^2}{90} T^4 + \frac{g^2\phi^2}{96} T^2 - \frac{g^3\phi^3}{96\pi} T + \cdots \Big) \ . \end{aligned} \tag{34}$$

Here the expression in brackets coincides with the contribution of a scalar field with mass m_W; the factor 2 appears since there are two W-bosons with opposite charges, while the factor 3, which will be particularly important in what follows, corresponds to the two transverse and one longitudinal degrees of freedom with mass m_W.

Alternatively, we can obtain the cubic term by looking directly at the one-loop Feynman diagrams. For this purpose, it is only necessary to examine the zero frequency contributions. Certain diagrams containing *four* external lines of the classical scalar field naively give a contribution proportional to $g^4\phi^4$; the cubic term arises because the zero frequency integrals diverge for small mass as $T/m_W \sim T/g\phi$.

Consider, in particular, the zero frequency part of the expression for the one loop free energy in momentum space. It is simplest to compute the tadpole diagrams for $dV/d\phi$, as indicated in Fig. 4, and afterwards integrate with respect to ϕ. The transverse gauge bosons give a contribution

$$\frac{dV_{\rm tr}}{d\phi} = 2 \times \frac{g^2\phi T}{2} \int \frac{d^3k}{(2\pi)^3} \frac{1}{\vec{k}^2 + m_W^2} = -2 \times \frac{g^2\phi\, T}{8\pi} \sqrt{m_W^2} \ , \tag{35}$$

where, by keeping only the zero frequency mode, we have dropped terms which are analytic in m^2.[4] The Coulomb lines give half the result of eq. (35). Integration of the total vector field contribution correctly represents the cubic term in (34).

A complete gauge boson contribution to the tadpole, including the non-

[4] The integral has been defined by dimensional regularization; ultraviolet divergences here are absorbed into the usual zero temperature renormalizations.

zero frequency modes, is [3]

$$\frac{dV_W(\phi,T)}{d\phi} = 2\times 3\times \frac{g^2\phi}{48}\left(T^2 - \frac{3m_W T}{\pi} + \cdots\right) = 2\times 3\times \frac{g^2\phi}{48}\left(T^2 - \frac{3\,g\phi T}{2\pi} + \cdots\right). \tag{36}$$

One can easily check that integration of this expression with respect to ϕ gives eq. (34).

With these techniques, we are in a good position to study higher order corrections to the potential. The authors of Refs. [23], [24] found a linear contribution to the potential by substituting the mass found at one loop back into the one loop calculation. The effective masses-squared of both scalar particles and of the Coulomb field contain terms of the form $\sim g^3 T\phi$, which, upon substitution in (34), give linear terms. But this procedure is not always correct. It is well known that the sum of the geometric progression, which appears after the insertion of an arbitrary number of polarization operators $\Pi(\phi,T)$ into the propagator $(k^2+m^2)^{-1}$, simply gives $(k^2+m^2+\Pi(\phi,T))^{-1}$. Therefore one can actually use propagators $(k^2+m^2+\Pi(T))^{-1}$, which contain the effective mass-squared $m^2+\Pi(\phi,T)$ instead of m^2. However, this trick with the geometric progression does not work for the closed loop diagram for the effective potential, which contains $\ln(k^2+m^2)$. A naive substitution of the effective mass squared $m^2+\Pi(\phi,T)$ instead of m^2 into $\ln(k^2+m^2)$ corresponds to a wrong counting of higher order corrections.

A simple way to take into account high temperature corrections to masses of vector and scalar particles without any problems with combinatorics is to compute tadpole diagrams for $\frac{dV}{d\phi}$; these are then trivially integrated to give the potential. One can easily check by this method that no linear terms appear in the expression for $V(\phi,T)$. Indeed, at a given temperature and effective mass, the tadpoles are linear in ϕ (see e.g. equation (36)). To take into account the mass renormalization in the tadpoles, one should substitute the effective mass squared $m^2+\Pi(\phi,T)$ into the one-loop expression for the tadpole contribution; as we explained above (see also ([3])), this is a correct and unambiguous procedure for tadpoles. Since $m^2+\Pi(\phi,T)$ is not singular in the limit $\phi\to 0$, the tadpole (36) in this limit remains linear in ϕ. Therefore its integration with respect to ϕ, which gives the correction to the effective potential, is quadratic in ϕ, *i.e.* it does not contain any linear

terms. [5]

Even though there are no linear terms $\sim g^3\phi T^3$, higher order corrections do have a dramatic effect on the phase transition, which has apparently not been noted before. This effect is a modification of the cubic term.

As we have shown above, the cubic term appears due to the contribution of zero modes, $\omega_n = 2\pi nT = 0$. This makes it particularly easy to study its modification by high order effects. Indeed, it is well known that the Coulomb field at zero frequency acquires the Debye 'mass', $m_D^2 = \Pi_{00}(\omega_n = 0, \vec{k} \to 0) \sim g^2\,T^2$. This leads to an important modification of the Coulomb propagator (30):

$$D_{00}(\vec{k} \to 0) = \frac{1}{\vec{k}^2 + m_D^2 + m_W^2(\phi)} \ . \tag{37}$$

For the values of ϕ of interest to us, $m_D^2 \gg m_W^2(\phi)$. Thus, repeating the calculation of the cubic term, the Coulomb contribution disappears. However, the transverse contribution, which is two times larger than the Coulomb one, is unaffected at this order, due to the vanishing of the 'magnetic mass'

[5]The absence of a linear term in ϕ can be understood in an effective Lagrangian approach as well. Such an approach automatically gives the correct combinatorics. Since, at weak coupling, we are interested in energy scales much less than πT, one can first integrate out all modes of the various fields with non-zero Matsubara frequency, thereby obtaining a three-dimensional effective action for the light fields. At one loop, one has the usual mass corrections, order g^2T^2 for the Coulomb and scalar lines, whereas the quadratic term for the transverse gauge bosons goes to zero with $\vec{k}$ and ϕ. These 'mass corrections' are analytic in $|\phi|^2$; in particular, they do *not* contain linear terms in ϕ. By assumption, the Higgs field is light at the phase transition, but one can again integrate out the massive Coulomb field. It is still true (as a consequence of gauge invariance) that the quadratic term for the transverse gauge bosons vanishes at zero momentum. Having done this procedure, we compute the effective potential for ϕ by calculating the determinant of Gaussian fluctuations in the low energy theory, i.e. the three dimensional theory containing only transverse gauge bosons and scalars. The linear terms in ϕ used in Ref. [24] come from loops of *light* fields ($\omega = 0$), and so in the present language we need to check that there is no non-analytic behavior in higher loop graphs in the effective theory. In fact, although individual diagrams may be singular, the sum of all two loop graphs is non-singular, essentially due to gauge invariance, and so the effective potential contains no linear term in ϕ, to this level of approximation. The cubic term is correctly reproduced by this process (see below).

[5, 35]. As a result, the cubic term does not disappear, but it is diminished by a factor[6] of 2/3: [7]

$$E = \frac{1}{6\pi v_o^3}(2m_W^3 + m_Z^3) \ . \tag{38}$$

This small correction proves to be very significant. Indeed, eqs. (15), (16) show that the ratio of the scalar field ϕ to the temperature at the moment of the phase transition is proportional to E, i.e. to the cubic term. Actually, the dependence is even slightly stronger, since for smaller E the tunneling occurs earlier. Results of a complete numerical investigation of the ratio ϕ/T at the moment of the phase transition, as a function of the Higgs boson mass are shown in Fig. 5, for the top quark mass $m_t = 120$ GeV. We have found that the ratio ϕ/T is not very sensitive to the mass of the top quark, in the interval 100 GeV $\lesssim m_t \lesssim$ 150 GeV, and it decreases for m_t outside this interval. Even before the reduction of the cubic term was taken into account, the ratio ϕ/T for $m_H \gtrsim 57$ GeV was slightly less than the critical value $\phi/T \approx 1$. The decrease of this quantity by a factor of 2/3 makes it absolutely impossible to preserve the baryon asymmetry generated during the phase transition in the minimal model of electroweak interactions with $m_H \gtrsim 57$ GeV.

Is this the end of the story? The effective coupling constant of interactions between W bosons and Higgs particles is $g/2$. In this case, a general investigation of the infrared problem in the non-Abelian gauge theories at a finite temperature suggests that the results which we obtained are reliable for $\phi \gtrsim \frac{g}{2} T \sim T/3$ [5], [35]. Thus, a more detailed investigation is needed to study behavior of the theories with $m_H \gtrsim 10^2$ GeV near the critical tem-

[6] We should point out that if the magnetic mass of the transverse gauge bosons were to be numerically rather large, then the factor E would be reduced further, leading to a further weakening of the order of the phase transition.

[7] After we obtained this result, we received a paper by Carrington [26] where the renormalization of the cubic term was also considered. A similar investigation was performed by Shaposhnikov as well [24]. These authors did not point out that they obtained the renormalization of the cubic term by the factor of 2/3, but after some algebra one can identify those terms in their expressions which are equivalent to ours. However, for different reasons, the final numerical results for the ratio ϕ/T obtained by both Shaposhnikov and Carrington differ from our result considerably, being approximately two times larger than our result shown in Fig. 5.

perature, since the scalar field, which appears at the moment of the phase transition in these theories, is very small (see Fig. 5). However, we expect that our results are reliable for strongly first order phase transitions with $\phi \gtrsim T$, which is quite sufficient to study (or to rule out) baryogenesis in the electroweak theory.

Finally, we would like to address a fundamental question: since the theory for $\phi \ll gT$ is infrared divergent, can we definitely establish that the symmetry is restored at high temperature, or is it possible that ϕ always has some small, non-zero value? To address this question, we can work at $T \gg T_o$. In this case, the scalar field is massive, and scalar loops are not singular in the infrared. Potential infrared problems arise only from gauge boson loops. For these, the situation is similar to that in high temperature QCD [35]. The standard assumption about QCD is that the infrared divergences are cut off at a scale $m_{mag} \sim g^2 T$ (the detailed mechanism of the infrared cutoff will not be important to us). The free energy, Ω, is non-singular through order $g^4\,T^4$. At order $g^6\,T^4$, there is a logarithmic infrared divergence; $\Omega \sim g^6\,T^4 \ln(m_{mag}/T) \sim g^6\,T^4 \ln g^2$. Higher order corrections go as $g^6\,T^4(g^2\,T/m_{mag})^n$, *i.e.* they are all of the same order. It is usually assumed, then, that the free energy can be computed through order $g^6\,T^4 \ln g^2$. A similar investigation suggests that the effective mass can be calculated with an accuracy $g^4\,T^2 \ln g^2$.

What are the consequences of these assumptions for the electroweak theory? First, the existence of an infrared cutoff of order $g^2\,T$ means that the potential is analytic in $|\phi|^2$, for small ϕ. This implies, in particular, that there are no linear terms in ϕ. Consider, then, the calculation of the ϕ^2 term, which determines the value of the critical temperature. At lowest order, one has the standard result, $DT^2\phi^2 \sim g^2T^2\phi^2$. At two loop order, there is a correction proportional to $g^4T^2\phi^2 \ln g^2$; higher order corrections all go as $g^4T^2\phi^2$. Thus, as in QCD, we can say that the mass term can be calculated to order $g^4T^2 \ln g^2$. This is a small correction, and the one-loop calculation is reliable: for small ϕ, the curvature of the potential is the sum of the (zero-temperature) negative term $-\frac{\mu^2}{2}\phi^2 + 2Bv_o^2\phi^2$, and a positive term $DT^2\phi^2 + O(g^4 \ln g^2)T^2\phi^2$ which grows with temperature. Thus, we have a phase transition, and the higher loop effects can only lead to corrections $\sim g^2 \ln g^2$ to the value of the critical temperature obtained in the one loop

approximation.

Note that this discussion is valid for any value of the Higgs mass. If these arguments are correct, then we expect the situation with the phase transitions in the non-Abelian gauge theories to be the same as in the standard case: infrared problems may prevent a simple description of the phase transition in a small vicinity of the critical point (unless the phase transition is strongly first order), but everywhere outside this region, the symmetry behavior of gauge theories can be described in a reliable way. We hope to return to a discussion of this interesting question in a separate publication.

5 Subcritical Bubbles

Despite our semi-optimistic conclusions concerning the infrared problem, it is still desirable to check that the whole picture of the behavior of the scalar field described above is (at least) self-consistent. This means that if the effective potential is actually given by eqs. (7), (8), (10), (11), (38), then our subsequent description of the phase transition and the bubble formation is correct. Indeed, one would expect that the theory of bubble formation is reliable, since the corresponding action for tunneling S_3/T is very large, $S_3/T \sim 130 - 140$. However, recently even the validity of this basic assumption has been questioned. Gleiser and Kolb [28] and Tetradis [29] have argued that in many cases phase transitions occur not due to bubbles of a critical size, which we studied in section 3, but due to smaller, subcritical bubbles. We believe that these authors raise a real issue. However, we will now argue that this problem only arises if the phase transition is extremely weakly first order.

The basic difference between the analysis of Ref. [28, 29] and the more conventional one is their assumption that at the time of the phase transition there is a comparable probability to find different parts of the universe in either of the two minima of $V(\phi, T)$. The main argument of Ref. [28, 29] is that if the dispersion of thermal fluctuations of the scalar field $< \phi^2 > \sim T^2$ is comparable with the distance between the two minima of $V(\phi, T)$, then the field ϕ "does not know" which minimum is true and which is false.

Therefore it spends comparable time in each of them. According to [28], a kind of equilibrium between the domains of the two types is achieved due to subcritical bubbles with small action S_3/T if many such bubbles may appear within a horizon of a radius H^{-1}.

In order to investigate this question in a more detailed way, let us re-examine our own assumptions concerning the distribution of the scalar field ϕ prior to the moment at which the temperature drops down to T_1, when the second minimum of $V(\phi, T)$ appears. According to (13), the value of the scalar field ϕ in the second minimum at the moment when it is formed is equal to $\phi_1 = \frac{3ET}{2\lambda_T}$. For $m_H \sim 60$ GeV (and taking into account the coefficient 2/3 in the cubic term) one obtains $\phi_1 \sim 0.4\,T$. Thermal fluctuations of the field ϕ have the dispersion squared $< \phi^2 >= T^2/12$. (Note an important factor 1/12, which was absent in the estimate made in [28].) This gives dispersion of thermal fluctuations $\sqrt{< \phi^2 >} \sim 0.3\,T$, which is not much smaller than ϕ_1.

However, as the authors of [28] emphasized in their previous work [36] (see also [29]), the total dispersion $< \phi^2 > \sim T^2/12$ is not an adequate quantity to consider since we are not really interested in infinitesimally small domains containing different values of fluctuating field ϕ. They argue that the proper measure of thermal fluctuations is the contribution to $< \phi^2 >$ from fluctuations of the size of the correlation length $\xi(T) \sim M^{-1}(T)$. This leads to an estimate $< \phi^2 > \sim T\,M(T)$, which also may be quite large [36]. Here again one should be very careful to use the proper coefficients in the estimate. One needs to understand also why this estimate could be relevant.

In order to make the arguments of Ref. [28, 29] more quantitative and to outline the domain of their validity, it is helpful to review the stochastic approach to tunneling (see [37] and references therein). This approach is not as precise as the euclidean approach (in theories where the euclidean approach is applicable). However, it is much simpler and more intuitive, and it may help us to look from a different point of view on the results we obtained in the previous section and on the approach suggested in [28, 29].

The main idea of the stochastic approach can be illustrated by an example of tunneling with bubble formation from the point $\phi = 0$ in the theory (22)

with the effective potential

$$V(\phi,T)=\frac{M^2(T)}{2}\phi^2-ET\phi^3+\frac{\lambda_o}{4}\phi^4. \tag{39}$$

For simplicity, we will study here the limiting case $\lambda_o \to 0$.

At the moment of its formation, the bubble wall does not move. In the limit of small bubble velocity, the equation of motion of the field ϕ at finite temperature is simply,

$$\ddot{\phi}=d^2\phi/dr^2+(2/r)d\phi/dr-V'(\phi)\ . \tag{40}$$

The bubble starts growing if $\ddot{\phi}>0$, which requires that

$$|d^2\phi/dr^2+(2/r)d\phi/dr|<-V'(\phi)\ . \tag{41}$$

A bubble of a classical field is formed only if it contains a sufficiently big field ϕ. It should be over the barrier, so that $dV/d\phi<0$, and the effective potential there should be negative since otherwise formation of a bubble will be energetically unfavorable. The last condition means that the field ϕ inside the critical bubble should be somewhat larger than ϕ_*, where $V(\phi_*,T)=V(0,T)$. In the theory (39) with $\lambda_o \to 0$, one has $\phi_*=M^2/2ET$. As a simplest (but educated) guess, let us take $\phi \sim 2\phi_*=M^2/ET$. Another important condition is that the size of the bubble should be sufficiently large. If the size of the bubble is too small, the gradient terms are bigger than the term $|V'(\phi)|$, and the field ϕ inside the bubble does not grow. Typically, the second term in (41) somewhat compensates the first one. To make a very rough estimate, one may write the condition (41) in the form

$$\frac{1}{2}r^{-2}\sim\frac{1}{2}k^2<\frac{1}{2}k_{max}^2\sim\phi^{-1}|V'(\phi)|\sim 2M^2. \tag{42}$$

Let us estimate the probability of an event in which thermal fluctuations with $T\gg M$ build up a configuration of the field satisfying this condition. The dispersion of thermal fluctuations of the field ϕ with $k<k_{max}$ is given by

$$\begin{aligned} <\phi^2>_{k<k_{max}} &= \frac{1}{2\pi^2}\int_0^{k_{max}}\frac{k^2dk}{\sqrt{k^2+M^2}\left(\exp\frac{\sqrt{k^2+M^2(\phi)}}{T}-1\right)} \\ &\sim \frac{T}{2\pi^2}\int_0^{k_{max}}\frac{k^2dk}{k^2+M^2}\ . \end{aligned} \tag{43}$$

Note that the main contribution to the integral is given by $k^2 \sim k_{max}^2 \sim 4M^2$. This means that one can get a reasonably good estimate of $< \phi^2 >_{k<k_{max}}$ by omitting M^2 in the integrand. This also means that this estimate will be good enough even though the effective mass of the scalar field $M^2(\phi) = V''(\phi)$ changes between $\phi = 0$ and ϕ. The result we get is

$$< \phi^2 >_{k<k_{max}} \simeq \frac{T}{2\pi^2} \int_0^{k_{max}} dk = \frac{T k_{max}}{2\pi^2} = \frac{C^2 T M}{\pi^2} \ . \tag{44}$$

Here $C = O(1)$ is a coefficient reflecting the uncertainty in the determination of k_{max} and estimating the integral.

Thus, we have a rough estimate of the dispersion of perturbations which may sum up to produce a field ϕ which satisfies the condition (42). We can use it to evaluate the probability that these fluctuations build up a bubble of the field ϕ of a radius $r > k_{max}^{-1}$. This can be done with the help of the Gaussian distribution[8]

$$P(\phi) \sim \exp(-\frac{\phi^2}{2 < \phi^2 >_{k<k_{max}}}) = \exp(-\frac{M^3\pi^2}{2C^2E^2T^3}) \sim \exp(-\frac{4.92M^3}{C^2E^2T^3}) \ . \tag{45}$$

Note that the factor in the exponent in (45) to within a factor of $C^2 = 1.02$ coincides with the exact result for the tunneling probability in this theory obtained by the euclidean approach [27] (see eq. (27)):

$$P \sim \exp(-\frac{4.85M^3}{E^2T^3}) \ . \tag{46}$$

Taking into account the very rough method we used to calculate the dispersion of the perturbations responsible for tunneling, the coincidence is rather impressive.

As was shown in [37], most of the results obtained in the tunneling theory by euclidean methods can easily be reproduced (with an accuracy of the coefficient $C^2 = O(1)$ in the exponent) by this simple method.

Now let us return to the issue of subcritical bubbles. As we have seen, dispersion of the long-wave perturbations of the scalar field, $< \phi^2 >_{k<k_{max}} \simeq$

[8]The probability distribution is approximately Gaussian even though the effective potential is not purely quadratic. The reason is that we were able to neglect the curvature of the effective potential $m^2 = V''$ while calculating $< \phi^2 >_{k<k_{max}}$.

$\frac{k_{max}\,T}{2\,\pi^2}$, is quite relevant to the theory of tunneling. Its calculation provides a simple and intuitive way to get the same results as we obtained earlier by the euclidean approach [37]. To get a good estimate of the probability of formation of a critical bubble in our simple model one should calculate this dispersion for $k_{max} \sim 2M(T)$, which gives $< \phi^2 >_{k<k_{max}} = TM/\pi^2$. Note, that this estimate is much smaller than the naive estimate $< \phi^2 > \sim TM$.

The crucial test of our basic assumptions is a comparison of this dispersion and the value of the field ϕ at the moment $T = T_1$, when the minimum at $\phi = \phi_1 \neq 0$ first appears. Using eqs. (7), (13), one can easily check that the mass of the scalar field at $T = T_1$, $\phi = 0$ is given by

$$m = \frac{3ET}{2\sqrt{\lambda_T}} \ . \tag{47}$$

This yields

$$\sqrt{< \phi^2 >}_{k<k_{max}} \ \sim \phi_1 \ \frac{\lambda^{3/4}}{\pi\sqrt{3E/2}} \approx \phi_1 \ \frac{10\lambda_T^{3/4}}{\pi} \ . \tag{48}$$

For the Higgs boson with $m_H \sim 60$ GeV one obtains

$$\sqrt{< \phi^2 >}_{k<k_{max}} \ \sim \frac{\phi_1}{5} \ . \tag{49}$$

Thus, even with account taken of the factor 2/3 in the expression for E, the dispersion of long-wave fluctuations of the scalar field is much smaller than the distance between the two minima. Therefore, the field ϕ on a scale equal to its correlation length $\sim M^{-1}$ is not equally distributed between the two minima of the effective potential. It just fluctuates with a very small amplitude near the point $\phi = 0$. The fraction of the volume of the universe filled by the field ϕ_1 due to these fluctuations (i.e. due to subcritical bubbles) for $m_H \sim 60$ GeV is negligible,

$$P(\phi_1) \sim \exp\left(-\frac{\phi^2}{2 < \phi^2 >_{k<k_{max}}}\right) \sim \exp\left(-\frac{3E\,\pi^2}{4\lambda_T^{3/2}}\right) \sim e^{-12} \ . \tag{50}$$

Since we already successfully applied this method for investigation of tunneling, we expect that this estimate is also reliable. The answer remains rather

small even for $m_H \sim 100$ GeV, when the phase transition is very weakly first order.

Moreover, even these long-wave fluctuations do not lead to formation of stable domains of space filled with the field $\phi \neq 0$, until the temperature is below T_c and critical bubbles appear. One expects a typical subcritical bubble to collapse in a time $\tau \sim k_{max}^{-1}$; this is about thirteen orders of magnitude smaller than the total duration of the phase transition, $\Delta t \sim 10^{-2} H^{-1} \sim 10^{-4} M_p T^{-2}$. We do not see any mechanism which might increase τ by such a large factor; effects such as decrease of the speed of the collapse of such bubbles due to finite-temperature effects (considered in the next section), or the inefficiency of radiating away the energy of oscillating subcritical bubbles [38] are much more modest.

Despite all these comments, we think that subcritical bubbles deserve further investigation. They may lead to interesting effects during phase transitions in GUTs, since the difference between T^{-1} and the duration of the GUT phase transitions is not as great as in the electroweak case. They may play an important role in the description of the electroweak phase transition as well, in models where the phase transition occurs during a time not much longer than T^{-1}. This may prove to be the case for very weakly first order phase transitions with $m_H \gtrsim 10^2$ GeV, when the distance between the two minima of $V(\phi, T)$ at $T \sim T_1$ is smaller than the dispersion $\sqrt{< \phi^2 >_{k<k_{max}}} \sim \sqrt{TM}/\pi$.

6 Propagation of the Bubble Wall

6.1 General Considerations

After bubbles are formed, one expects that they will grow until they collide. Since the expansion rate is so small at this time, provided the bubbles have a velocity which is not *extremely* small, typical bubbles will grow to a macroscopic size. Thus, it is important to understand how bubbles propagate long after their formation. An underlying assumption in discussions of the evolution of the bubble wall to date is that some time after the forma-

tion of the bubble, a steady state situation is achieved, in which the scalar field, temperature, and particle velocities are all constant in time in a frame which we will call the 'wall frame.' While it is plausible that such a state is achieved, we will not prove that this is the case; indeed, as we explain below, one can imagine situations in which this is not the case. To develop some intuition, we will consider two simple models. One picture, which suggests that a steady state will arise, is the following. As the wall passes through the medium, it dissipates energy and heats the gas. Since the wall is quite permeable, especially to light quarks, heat is readily transported both behind and in front of the wall. Once the wall is very large, the problem becomes one dimensional, so consider as a model a point source of heat, moving in an incompressible fluid with velocity v. The temperature will obey a diffusion equation, with diffusion coefficient χ. The solution of this equation is

$$T - T_\infty = \frac{q}{v\sqrt{\chi}} \int_{-\infty}^{0} \frac{dx'}{\sqrt{x'}} \exp\Big(v\frac{(x - x' - vt)^2}{4\chi x'}\Big) , \tag{51}$$

where T_∞ is the temperature as $x \to \infty$. Note that this is a function only of $x - vt$, so that in the wall frame one has a steady distribution. χ is of order a mean free path, ℓ. Thus, if v is small, the temperature varies on a scale of order ℓ/v, i.e. on a scale large compared to a mean free path, ℓ.

Thus, it seems plausible that a steady state situation is achieved. However, L. Susskind has given a simple example in which this is not the case, which we refer to as a 'snowplow.' Suppose one has, in the original, unbroken phase, a non-zero density of some exactly conserved quantum number; we will refer to these particles as 'molecules.' Suppose also, that the molecules have a big potential energy in the broken phase. Then it is easy to convince oneself that there is no steady solution; necessarily, there must be a build up of molecules as time evolves. Indeed, one might guess that in this case there is a layer of molecules in front of the wall, which grows in size linearly with time. Moreover, viewed in the frame of the wall, there is a steady 'wind' of particles. These particles collide with the ever growing layer of molecules, which is stationary in the frame of the wall. The molecules in this wind, presumably, equilibrate, so the wind comes to rest in the wall frame. This buildup of particles leads to an increase in pressure near the wall of order ρv^2, where ρ is the molecule density and v the velocity. Balancing the stresses on

the wall then gives

$$v^2 \sim \frac{\delta p}{\rho} \ . \tag{52}$$

Note that it is important, in determining the force on the wall, that the properties of the gas near the wall depend on the velocity of the wall.

In the Standard Model, there is no exactly conserved quantum number of this type. However, there are several approximately conserved quantum numbers, and one can ask whether something like this snowplow effect can occur. Again to develop some intuition, it is helpful to consider a simple model. Imagine a wall passing through a region of 'sticky dust.' The dust particles, when struck by the wall, stick to it, but after they hit the wall they have a lifetime τ. Then the number of particles per unit area on the wall, N, satisfies

$$\frac{dN}{dt} = n_0 v - \frac{1}{\tau} N \ , \tag{53}$$

where n_0 is the density of particles and v is the wall velocity. For a steady state, $N = n_0 v \tau$. In our case, the analog of the dust particles are top quarks, and the lifetime τ is some characteristic time to change the number of tops and antitops (we will discuss this in more detail below). Thus, we do in fact expect some velocity-dependent enhancement of the top quark density near the wall, but we do not expect that the layer out front should grow indefinitely. For the rest of this paper, we will assume that the wall does indeed achieve a steady state. On the other hand, as we will discuss shortly, the enhancement of the density we have discussed above may be an important factor determining the wall velocity.

Turok [30] has argued that reflection of particles from the wall does not slow the wall's motion. His argument starts with the (correct) observation that if the velocity and temperature of the gas are constant across the wall, and if everywhere the system is described by equilibrium distributions appropriate to the local value of ϕ, the force on the wall is independent of the velocity. It is instructive to consider this part of the argument, and indeed a modified version of the method for estimating the force on the wall will be useful in our analysis.

In the wall frame, the net force on the gas is simply

$$\frac{dP^i}{dt} = \int d^3x \; \frac{d^3k}{2k^0(2\pi^3)} \, n(\vec{k},\vec{x}) \, \frac{\partial m^2}{\partial x} \; . \tag{54}$$

With the assumption that the velocity and temperature of the gas are nearly uniform across the wall, the density in the wall frame is simply the Lorentz-boosted distribution from the gas frame. On the other hand, $n(\vec{k},\vec{x})$ transforms as a Lorentz scalar. Since $\frac{d^3k}{2k^0(2\pi^3)}$ is the Lorentz-invariant volume element, a simple change of variables gives for the net force a result independent of the wall velocity. From this Turok concludes that one needs to find other sources of dissipation if the wall is not to accelerate continuously.

Our earlier discussion suggests, however, that the particle distributions near the wall will exhibit a more complex dependence on the wall velocity. In other words, even for small velocity, there will be departures from equilibrium proportional to the velocity. In the following sections, we will try to take this velocity-dependence into account, and estimate the damping of the wall's motion due to scattering of particles from the wall. There will, of course, be other sources of damping; in some regimes, these may be larger. However, we will see that from this source alone, damping is sufficient to give non-relativistic motion of the wall for a wide range of parameters.

The calculations which follow make use of the infrared improved effective potential described in Section 4 for which, as already pointed out, baryogenesis has been ruled out experimentally. However, the study of the propagation of the bubble wall in a hot plasma receives its main motivation from the understanding of the baryogenesis at the weak scale. We will consequently use the above potential as a toy model in a range of parameters so chosen that baryogenesis is a viable phenomenon. To this end, we will often use in what follows the value $m_H = 35$ GeV for which $\phi/T \gtrsim 1$.

6.2 Three Limiting Cases

This discussion suggests that there are three limiting cases which one might wish to consider. In the first, the wall is thin compared to mean free paths for all scattering processes, both elastic and inelastic. Then a typical particle,

as it passes through the wall, loses momentum chiefly through its interaction with the wall. Near the wall, one expects significant, v-dependent departures from equilibrium. A second extreme will occur if the mean free paths for both elastic and inelastic processes are short compared to the size of the wall. In that case, the system will be quite close to equilibrium; deviations from equilibrium will be proportional to the velocity and some power of a typical mean free path. Finally – and this is the situation which we will see is closest to reality – mean free paths for elastic processes may be short, but for inelastic processes long. In this case, in addition to the small deviations from equilibrium we have just mentioned, there will also be a density enhancement as in our snowplow discussion. We expect that the wall will be slowest if the 'thin wall' picture is valid, fastest in the 'very thick wall' case (where mean free paths for inelastic processes are short) and will have some intermediate velocity in the third case.

In this and the following two sections, we will consider these three cases. After estimating the relevant length scales, we will make a series of (admittedly preliminary) computations of the velocity and wall thickness. We will see that all three limits suggest a non-relativistic value of the wall velocity.

Before considering the properties of the bubble wall, it is useful to consider the system at the critical temperature, T_c. At this temperature[9] it should be possible for the phases with broken and unbroken gauge symmetry to coexist. Regions of different phases should be separated by a wall, which we refer to as a bubble wall or domain wall, at rest. It is easy to determine the form of this bubble wall. One is looking for a static solution of the equations of motion in the presence of the gas; the relevant equation is simply

$$\frac{\partial^2 \phi}{\partial x^2} = \frac{\partial V(\phi, T)}{\partial \phi} \ . \tag{55}$$

We require that ϕ tend to a constant as $x \to \pm\infty$, so we can immediately solve the equation by quadrature:

$$\Delta x = \int \frac{d\phi}{\sqrt{2V(\phi, T)}} \ . \tag{56}$$

[9]We note that the analysis of Ref. [30] is indeed valid *at* $T = T_c$.

For a Higgs mass of 35 GeV, and a top quark mass of 120 GeV, one finds that the wall thickness is

$$\delta \sim 40\, T^{-1} \ . \tag{57}$$

This estimate of the wall thickness will provide a useful benchmark in what follows.

Indeed, it is useful to compare this number with the mean free paths for various processes. In considering the properties of the bubble wall, the relevant mean free paths are those for particles which interact with the wall, i.e. principally top quarks, W's and Z's. The processes with the shortest mean free paths are elastic scatterings. These exhibit the characteristic singularities of Coulomb scattering at small angles. What actually interests us, however, is the momentum and energy transfer in these collisions. This is a problem which has been extensively studied, and we can borrow the relevant results. For a relativistic top quark of energy E, one has [39]

$$\frac{dE}{dx} \sim -\frac{8\pi}{3}\alpha_s^2 T^2 \ln(E/T) \ . \tag{58}$$

We expect a similar formula to hold for W and Z scattering, with α_s replaced by α_W. This number is to be compared with the momentum loss due to interaction with the wall:

$$\frac{dp_x}{dx} = -\frac{1}{2p_x}\frac{dm^2}{dx} \ . \tag{59}$$

Assuming that the wall thickness is of order $\delta \sim 40\, T^{-1}$, and noting that for the t quark, $\Delta m^2 \sim .3\, T^2$, while for the W and Z, $\Delta m^2 \sim .2\, T^2$, one sees that the momentum loss per unit length due to scattering is in both cases much larger than that due to the wall.

We can understand this result in an alternative way. The elastic scattering cross section diverges at small angles, in empty space. In the plasma, we expect that this divergence is cut off. Examining the expression for the gluon propagator in Ref. [40], we see that for the Coulomb fields, this cutoff is the Debye mass,

$$m_D^2 = (2N_c + N_f)\ \frac{g_s^2 T^2}{6} \approx\ 2.5 T^2 \ , \tag{60}$$

while for transverse gauge bosons, it is $m_D^2 k_0^2/3k^2$. Actually, the fact that m_D is comparable with T means that one should go back and self-consistently calculate the propagators (more or less as we did in our discussion of the Higgs potential earlier). We will not do this here, but instead simply assume that both the transverse and longitudinal gauge boson exchanges are cut off at a scale of order T. So to get a crude estimate of the mean free path, we simply calculate the elastic scattering cross section with a gauge boson propagator

$$D_{\mu\nu} = \frac{g_{\mu\nu}}{q^2 - T^2} \ . \tag{61}$$

One then obtains a total cross section

$$\sigma_t \simeq \frac{16\pi\alpha_s^2}{T^2} \ . \tag{62}$$

To estimate the mean free path, we multiply this by the flux of quarks. Similarly one can estimate the contribution due to scattering from gluons, and the mean free paths of W's and Z's. Finally one obtains an estimate for the mean free path of order $\ell \sim 4\,T^{-1}$ for quarks, and $\ell \sim 12\,T^{-1}$ for W's and Z's. We will see below that the wall velocity goes as $\sqrt{\ell}$; we expect that the uncertainties here will not qualitatively affect those calculations. It would be desirable to redo this analysis including the screening self-consistently and using real transport equations. However, it is reassuring that they are consistent with the expression above for the stopping power.

We will also need an estimate of the mean free path for processes which change the number of top quarks or the number of W's and Z's. A good measure of this distance is provided by the lifetimes of these particles in the high temperature plasma. If we treat the scalar field as approximately constant in space, then we expect that these decay rates have essentially the same form as the zero temperature rates, with the zero-temperature masses replaced by ϕ-dependent masses, and including the appropriate factor for time dilation. Hence the ratio of widths to masses is the same as at zero temperature, weighted by the Lorentz factor. These give numbers of order 1% or smaller and thus the mean free path for decays will be of order 100's of T^{-1}'s. While we have not attempted to do a complete analysis, it appears from an examination of many cross sections that processes which equilibrate the various types of particle numbers are not likely to be effective at distances of order δ.

6.3 Thin Wall

The first limiting case we will consider, in some ways conceptually the simplest, is what we refer to as the 'thin wall.' In this limit, the thickness of the wall, δ, is less than a typical mean free path ℓ for relevant particles.[10] In particular, the momentum transferred by scattering to top quarks, W's and Z's (the particles which gain mass in the broken phase) as they pass through the wall is small compared to the change in their mass. These particles constitute roughly 20% of the plasma. The other 80%, made up of light particles, are irrelevant in the sense that they interact only very weakly with the wall, but play an active role in establishing a steady state. In this limit, one can compute the force on the wall semiclassically by assuming some distribution on either side, and then simply following trajectories of individual particles across the wall. In the rest frame of the wall, energy is conserved, so it is easy to compute the momentum transferred by individual particles to the wall as they pass through or are reflected back. To estimate the force on the wall in this case, we will take advantage of the one dimensional geometry of the problem, and suppose that the wall is moving in the $+x$ direction with velocity v. We will assume that the wall is surrounded by a plasma of roughly constant temperature and velocity. Indeed, our discussion of the diffusion equation (51) suggests that the temperature and other quantities should vary on a scale ℓ/v. For small wall velocity, this is much larger than the thickness of the wall. This assumption will be justified *a posteriori*.

We noted in the first section of this paper that a simple estimate, eq. (1), was obtained in Ref. [27]. This estimate is valid for strongly first order phase transitions, when the main difference in energy density ρ inside and outside the bubble is due to heavy particles, which acquire mass $m \gg T$ inside the bubble. Such particles, coming from the phase $\phi = 0$, are completely reflected by the bubble wall. However, in the minimal electroweak theory, the masses of the particles are not very large compared to the temperature and one cannot neglect the effect of particles crossing the wall. We have presented full details of the calculation in the Appendix. We quote the results here,

[10] This should not be confused with the thin wall approximation during the bubble formation, when the thickness of the wall is assumed to be small as compared with the radius of the bubble.

obtained by expanding in small v:

$$v\mathcal{E} + \mathcal{O}(v^2) = V(0,T) - V(m,T) \ . \tag{63}$$

Here

$$\mathcal{E} = \rho(0,T) - \rho(m,T) - \frac{m^2}{4\pi^2}\int_m^\infty E\, n_o(E)\, dE \ . \tag{64}$$

In the limit of large masses ($m \gg T$), the last term in this equation vanishes and the first two accounts for the energy density contrast $\Delta\rho(0,T)$, in agreement with (1). To study the properties of eqs. (63), (64) further, we make an expansion in powers of m/T. After a little algebra, we obtain

$$\mathcal{E} = \frac{3}{\pi} E\, T\phi^3 + \frac{1}{4}\phi^4 \left[\lambda - \lambda_T + 2B\Big(4\ln\frac{\phi}{v_o} - 7\Big)\right] \tag{65}$$

and

$$V(0,T) - V(m,T) = -\left(\frac{T}{T_c} - \frac{\phi_c}{\phi}(1-\epsilon)\right)\frac{\lambda_{T_c}}{8}\phi_c\phi^3 \ , \tag{66}$$

with ϵ given by

$$\epsilon = \frac{T_c^2 - T^2}{T_c^2 - T_o^2} \simeq \frac{T_c - T}{T_c - T_o} \ . \tag{67}$$

In the case of small ϵ, when T is close to T_c and $\phi \sim \phi_c(1+\epsilon)$, eq. (63) gives

$$v \simeq \frac{\pi}{6}\frac{\epsilon}{1+\epsilon}\left(1 + \frac{\pi}{6}(1+\epsilon)\left[\frac{\lambda - \lambda_T}{\lambda_T} + \frac{2B}{\lambda_T}\Big(4\ln\frac{\phi}{v_o} - 7\Big)\right]\right)^{-1} \ . \tag{68}$$

The relevant value of ϵ corresponds to the time when the biggest bubbles propagate in the plasma, which is also the time when bubbles fill up the universe. Fig. 6 shows that ϵ varies between 0.1 and 0.3 for a large range of Higgs masses and is rather insensitive to the top mass; we use the value 0.26 corresponding to a Higgs mass of 35 GeV to illustrate our results. For a zero top mass,[11] the term in parenthesis is approximately 1; in such a case,

$$v \sim \frac{\pi}{6}\frac{\epsilon}{1+\epsilon} \sim 0.1 \ . \tag{69}$$

[11]This is clearly an unphysical value. However, this information will be useful in the discussion of thick walls in the next subsection, since for thick walls the top quark contribution is relatively suppressed.

As the top mass increases to a value $> m_Z$, its contribution becomes dominant and the velocity decreases significantly; as an example, for $m_t = 120$ GeV, $v \sim 0.06$. We have analyzed eq. (63) numerically, Fig. 7 shows the dependence of the velocity on ϵ while Fig. 8 illustrates the dependence of the velocity on the top mass.

We now elaborate further on the situation describing the steady state. Since particles change their momentum in crossing or bouncing off the wall, the local thermal distribution is spoiled; its restoration requires the release of energy-momentum at a certain rate, implemented by the flow of light quarks. Clearly, to satisfy the conservation of energy and momentum, the plasma has to adjust its velocity and temperature distributions. For this purpose, the wall and the non-thermalized particles can be viewed as a source of energy-momentum of a size of a few mean free paths, moving in a relativistic plasma with a non-relativistic velocity. This situation is similar to the diffusion problem described in Section 6.1. Qualitatively, one expects a steady state situation in the rest frame of the source, a rather uniform distribution of temperature and velocity behind the source extending across the source on a typical distance $l_D \sim \frac{\ell}{v}$. From our estimate of the velocity above, l_D is typically 20 times larger than ℓ which justifies the assumption that the wall is interacting with a plasma of uniform velocity and temperature. Furthermore, as a good approximation, we can assume this velocity and temperature to be the ones far away from the wall. We can then write equations for the conservation of energy and momentum across the wall:

$$\begin{aligned} \gamma'^2\Big(v'^2\rho(m,T') - V(m,T')\Big) - \gamma^2\Big(v^2\rho(0,T) - V(0,T)\Big) = 0 \ , \\ \gamma'^2 v'\Big(\rho(m,T') - V(m,T')\Big) - \gamma^2 v\Big(\rho(0,T) - V(0,T)\Big) = 0 \ , \end{aligned} \tag{70}$$

where $v' = v + \delta v$ and $T' = T + \delta T$ are the quantities defined behind the wall.

It is easy to compute the changes in velocity δv and temperature δT of the plasma as it crosses the wall. These equations and the steady state assumption, together with equation

$$\Big(V(0,T') - V(m,T')\Big) - v'\mathcal{E}' \simeq 0 \ , \tag{71}$$

yield a unique answer for these quantities. Typically, $\frac{\delta v}{v} \sim +1\%$, so the velocity, v, is still given accurately by Fig. 7. For the temperature variation,

one finds $\frac{\delta T}{T}$ is negative and of the order of or less than -0.0001%.[12] Furthermore, δv is positive; the process is a deflagration. It is also easy to check that a small amount of entropy is produced in the plasma, in agreement with the second law of thermodynamics.

One can attempt to obtain the shape of the wall by writing eqns. (70), (71) in a differential form. At $\epsilon = 0$, the resulting equation is just that which we studied earlier for the domain wall separating the coexisting phases. At finite ϵ, however, there are velocity-dependent corrections to the equation, and it is more difficult to analyze. Because the temperature and velocity vary in space, the problem one has to solve is analogous to the motion of a particle in a time-dependent potential. Moreover, the two minima of this potential are not degenerate, so one needs to understand how the oscillations of the scalar field in the true minimum are damped. However, for small ϵ (and v), we do not expect the shape of the wall to be too much different than for $\epsilon = 0$; in particular, the size of the wall (see eq. (56)) is still given to a good approximation by

$$\delta \sim 2\,\frac{\sqrt{2\lambda_T}}{E} \sim 40\ T^{-1}\ . \tag{72}$$

As this is a several times bigger than the mean free paths of the relevant particles ($\ell_{W,Z} \sim 12\,T^{-1}$ and $\ell_{top} \sim 4\,T^{-1}$), the thin wall approximation just described is questionable within the minimal version of the electroweak theory. However, this approximation may be valid in some extension of the standard model. For instance, the authors of Ref. [22] have argued that baryogenesis at the weak scale is viable in a model with a singlet scalar and one Higgs doublet. The presence of a light singlet makes the transition more strongly first order, and, consequently, allows for a Higgs mass above the experimental bound. In such models, the wall tends to be thinner.

So far, we have assumed for our thin wall analysis that the density to the left and right of the wall (of particles moving to the right and left, respectively) are precisely the equilibrium densities. However, our discussion earlier of the snowplow problem suggests that there may be other effects we should consider as well. Suppose that there were only elastic processes, i.e.

[12]The gradient of temperature, $\frac{\delta T}{T}$, goes like $\frac{\delta\gamma}{\gamma} \sim -v\delta v$.

no processes which changed the separate numbers of different particles and antiparticles. Suppose, also, that (for example) all top quarks were reflected from the wall. Then we would be in precisely the snowplow situation, except now in a relativistic version.

More realistically, consider the possibility that, say for top quarks, the probability of reflection from the wall of a given quark is f. Suppose, also, that the mean free path for processes which change the number of tops or anti-tops is τ. Then there will be some buildup of top quarks near the wall. The time required for the wall to catch up with a given top quark goes as $\frac{\ell}{v^2}$, where l is a typical mean free path. As a result, in the limit of very small v, the wall doesn't catch up with a typical particle before it undergoes an "identity change." Thus, we have something like the "sticky dust" picture described earlier. Per unit area of the wall, there is an increase in the number of top quarks of order $\tau f v n$, where n is the equilibrium top quark density. These quarks are spread over a distance of order $\sqrt{\ell\tau}$, so their density is of order $fvn\sqrt{\frac{\tau}{\ell}}$. This gives an extra contribution to the force on the wall of order $v\Delta\rho n f\sqrt{\frac{\tau}{\ell}}$, where $\Delta\rho$ is the free energy difference on the two sides of the wall. It is easy to compute f; for bosons, $f = \frac{\zeta(2)}{2\zeta(3)}\frac{m}{T}$; for fermions, the result is 2/3 as large. Assuming that the square root in this expression is a number of order 5-10, this is comparable to the force we have computed above, and will tend to decrease the velocity of the wall. This discussion, of course, is extremely crude, but it suggests that there are various effects at least as large as those we have considered above, all of which slow the wall. Thus, if the thin wall approximation is a good guide, the wall is likely to be quite non-relativistic. We will see that there are similar effects in the the case of a thicker wall.

6.4 Thick Wall

We now consider the case that the wall is extremely thick. As is clear from our earlier discussion of mean free paths, this, like the thin wall case, is not completely realistic. These calculations, however, should bracket the true situation. At the end of this section we will try to estimate the effects of the density enhancement which occurs because particle numbers are approx-

imately conserved. So we first consider the case where the mean free paths for both elastic and inelastic processes are short. To get an idea of how finite elastic scattering lengths affect the velocity of the bubble wall, we assume that particles propagate freely over distances of order a mean free path, ℓ. We view the bubble wall as a succession of slices with thickness of order ℓ, and for each of these we repeat the thin wall analysis. We refer the reader to the Appendix for the details of the derivation and the precise formulae, and just summarize the results here. We write the result in the following form

$$\mathcal{E} = \mathcal{S}_b \mathcal{E}_b^{thin} + \mathcal{S}_f \mathcal{E}_f^{thin} \ , \tag{73}$$

where $\mathcal{S}$ are suppression factors dependent on ℓ. They are not very sensitive to m_t and m_H, and behave as $(\ell/\delta)^{1/2}$ (see Fig. 9). Using the values quoted above ($\ell_{W,Z} \sim 12\,T^{-1}$, $\ell_{top} \sim 4\,T^{-1}$ and $\delta \sim 40\,T^{-1}$), we find $\mathcal{S}_b \sim 0.45$ and $\mathcal{S}_f \sim 0.15$. Using the equations for $\mathcal{E}$ from the previous section and assuming $m_H \sim 35$ GeV and $m_t \sim 120$ GeV, we find a velocity of about

$$v \sim 0.2 \ . \tag{74}$$

Using the values above for $\mathcal{S}_b$ and $\mathcal{S}_f$, Fig. 10 illustrates the velocity for a range of top masses.

In reality, however, we expect, because the numbers of tops and anti-tops (and similarly W^+'s and W^-'s) are not quickly equilibrated, their densities will be enhanced near the wall; since this enhancement will depend on the velocity, there will be a velocity-dependent drag on the wall, similar to that we discussed above in the thin wall case.

Again, we will content ourselves with an extremely crude estimate. As in the thin wall case, we imagine that as particles pass through the wall, some fraction is reflected. These reflected particles make a random walk until they decay, or undergo scattering processes which change their identity, with a lifetime τ. Then the number of particles per unit area on the wall is $N = fnv\tau$, where as before, f is the fraction of particles which are reflected. This extra density of particles will be spread over the thickness of the wall, or over $\sqrt{\ell\tau}$, whichever is larger. For our crude estimate, we will assume this density is spread uniformly over the wall. In other words, we will assume that the density is the equilibrium density (for a given value of the scalar field),

except enhanced by a factor of the form $1 + \frac{n_0 v \tau}{\ell}$. In this case, one obtains an increase force on the wall of order $\Delta F = \frac{f n v \tau}{\ell} \times \Delta\rho$, where, as before, $\Delta\rho$ denotes the internal energy difference on the two sides of the wall. As an estimate of the quantity f, we take the ratio of the equilibrium densities on the two sides of the wall. For top quarks, this gives a number of order 5%. The ratio $\frac{\tau}{\ell}$ is likely to be of order $5 - 10$. Thus, this effect may be even more important than the effects we have considered above, i.e. we have probably overestimated the wall velocity.

We can also ask about the wall thickness in this limit. Our discussion here suggests that the thickness will be modified from its value at T_o by a factor of the form $1 + \frac{n_0 v \tau}{\ell}$, i.e. by a small amount. However, it is somewhat harder to develop a complete theory of the wall shape in this limit. For example, in the analog mechanics problem, if one allows for spatial variation of the temperature, one has to consider a system with time-dependent forces. Moreover, one has to consider how the 'motion' of ϕ damps out in the region of broken symmetry. This may require consideration of types of damping other than those we have considered up to now. We will not explore this issue further here, and simply assume that the shape of the wall is only slightly modified from its form at T_c.

7 Conclusions

The study of the electroweak phase transition began two decades ago, and stimulated work in many areas of what has come to be called astroparticle physics. However, until now it was not very important to know any details of the theory of this phase transition. For most applications it was quite sufficient to know that in the early universe at a temperature higher than about 10^2 GeV the symmetry between weak and electromagnetic interactions was restored. Recently it has become clear that if we wish to investigate the possibility of electroweak baryogenesis, we must have a complete and detailed picture of the phase transition, from the accurate computation of the critical temperature to the investigation of the motion of the bubble walls. In this paper, we have taken some steps towards a systematic investigation of all relevant features of the first order phase transitions in electroweak theory.

We have seen how to organize the perturbation expansion in light of the infrared problems which exist at high temperature. We have shown that no dangerous linear terms arise in the effective potential; on the other hand, we have seen that the coefficient of the cubic term, which is responsible for the first order nature of the transition, is reduced by a factor 2/3 from its lowest order value. This means, in particular, that theories with a single Higgs doublet cannot be responsible for the observed baryon asymmetry, given the present experimental limits on the Higgs mass.

We have also understood some aspects of the strongly first order phase transition relevant to baryogenesis. For such theories, we have seen that the phase transition typically proceeds through the formation of critical bubbles with thick walls. We have developed a method of analytic investigation of the probability of bubble formation, which is valid for a large class of theories. With the help of the stochastic approach to tunneling, we have found that subcritical bubbles are only likely to be important (in the minimal standard model) for Higgs mass larger than about 100 GeV, when the phase transition is second order or very weakly first order.

We have considered the problem of propagation of the bubble wall. To this end, we have considered the minimal Higgs model with a light Higgs ($m_H < 35$ GeV). While this possibility is ruled out, we believe this theory is a good toy model, whose features mimic those of more realistic theories in which baryogenesis is possible. Investigation of the bubble wall motion turns out to be surprisingly difficult; indeed, we have identified important mechanisms for slowing the wall which have been omitted from previous treatments. Our own treatment is crude, and may omit additional damping effects, but it suggests that the bubble wall is typically non-relativistic or only mildly relativistic in these theories, and tends to be rather thick. It would be interesting to construct theories where this is not the case, which might realize the scenario of ref. [17] in which baryons are produced quite efficiently.

While in this paper we have seen that theories with a single Higgs doublet cannot give rise to the observed asymmetry, there is still much work to be done to determine whether or not baryogenesis can occur in extensions of the minimal theory. Needless to say, such extensions are interesting in their own

right, and also because they can provide larger CP violation than exists in the minimal model. Apart from the issues of the phase transition discussed here, further work on B-violation rates and the detailed mechanisms of baryon production is still necessary. Hopefully the observations contained in this paper will represent a positive step on the road to a complete understanding.

Acknowledgements

We are grateful to many of our colleagues for sharing their insights into these problems. In particular, we thank Lenny Susskind for discussions of the wall propagation, and suggesting we consider the "snowplow" problem, and Renata Kallosh for explaining to us some features of gauge fixing in spontaneously broken theories. We also thank Larry McLerran, Neil Turok and Marcelo Gleiser for discussing their work with us.

8 Appendix: Calculations of the Wall Velocity

In this appendix we give the details of our calculation of the force exerted on the advancing bubble wall by the plasma. As discussed in the text, we will assume that there exists a steady state; that is, there is a well-defined rest frame of the wall, at sufficiently late times after the appearance of the bubble. In this frame, we have a (time-independent) velocity and temperature distribution for each component of the plasma that reduce to those of the surrounding Universe at spatial infinity. We focus on those species that are relatively heavy in the broken phase; these will obviously give the greatest contribution.[13]

In principle to solve this problem in all generality, we would write Boltzmann equations for each component of the plasma, as well as an equation of motion for the scalar fields. However, in the simplest cases, we can learn a great deal by looking at the equations for local energy-momentum conservation. These may be written in the form

$$\partial_\mu T_\phi^{\mu\nu} + \partial_\mu T_{\rm gas}^{\mu\nu} = 0 \ , \tag{A.1}$$

where we have (arbitrarily) separated off the classical (zero-temperature) stress tensor of the scalar field. We can also write

$$-F_x^{(i)} = \partial_x T_{(i)}^{xx} \ , \tag{A.2}$$

where (i) labels components of the plasma and $F_x^{(i)}$ is the force density on the wall of the $i^{\rm th}$ species. Combining (A.1) and (A.2), we find the full equation for the scalar field:

$$\partial_\mu T_\phi^{\mu x} = \sum_i F_x^{(i)} \ . \tag{A.3}$$

We now turn to the evaluation of F_x.

Consider a volume element of width s in the x-direction. For our analysis, we will assume that particles of the plasma typically traverse this distance

[13]The light degrees of freedom can not be ignored however, as they are instrumental in the approach to and establishment of local kinetic equilibrium.

without interacting; we can calculate the force on this slice of the bubble wall by following individual particles of the distribution. We will present the analysis for a general s below, but note now that the size of s distinguishes the three cases considered in the text. Namely, the thin wall scenario corresponds to $s \sim \delta$, where δ is the wall thickness, the very thick wall corresponds to s infinitesimal, and the intermediate scenario to $s \sim \ell$, with ℓ some relevant mean free path. We will suppose that particles entering the volume element on either side are described by equilibrium distributions appropriate to the masses on either side (m_o or m_1, with $m_1 > m_o$). Note that particles leaving the volume element will not, in general, be thermally distributed; we assume that equilibrium is restored in a distance of order a mean free path. In other words, for particles entering the volume, we are assuming the distribution

$$n(E) = n_o\Big(\gamma_v(E - vp_x), T, \mu\Big) \ . \tag{A.4}$$

with $E = \sqrt{\vec{p}^2 + m_{o,1}^2}$.

We compute the force per unit area as follows. In time dt, there are $n(p,T)\frac{d^3p}{(2\pi)^3}|v_x|dt$ particles per unit area providing a force $\Delta p_x/dt$. Thus, the pressure is

$$dP = \int \frac{d^3p}{(2\pi)^3} n(p,T)(\Delta p_x)|v_x| \ . \tag{A.5}$$

We write the integration measure as $dE\ E\ dp_x/4\pi^2$. There are various regions of integration, corresponding to whether the particles have sufficient momentum ($p_x^2 > (m_1^2 - m_o^2)$) to go through the slice, or are reflected.

For particles bouncing off the wall, incident from the right, the momentum transfer is just $-2p_x$. We arrive at

$$\Delta P_I = \frac{2}{4\pi^2} \int dE\ dp_x\ p_x^2 n_o\Big(\gamma_v(E - vp_x), T\Big) \ , \tag{A.6}$$

where the region of integration is $[(m_o, m_1) \times (-\sqrt{(E^2 - m_o^2)}, 0)] + [(m_1, \infty) \times (-\sigma, 0)]$ with $\sigma = \sqrt{m_1^2 - m_o^2}$.

For particles incident from the right with $|p_x| > \sigma$, we find $\Delta p_x = -\sqrt{p_x^2 - \sigma^2} - p_x$ and the pressure is

$$\Delta P_{II} = \int \frac{dE}{4\pi^2}\ dp_x\ p_x \left(p_x + \sqrt{p_x^2 - \sigma^2}\right) n_o\Big(\gamma_v(E - vp_x), T\Big) \ , \tag{A.7}$$

where the region of integration is $[(m_1,\infty)\times(-\sqrt{(E^2-m_o^2)},-\sigma)]$.

For particles incident from the left, the momentum transfer is $\Delta p_x = \sqrt{p_x^2+\sigma^2}-p_x$ and so

$$\Delta P_{III} = \frac{1}{4\pi^2}\int dE\; dp_x\; p_x\left(-p_x+\sqrt{p_x^2+\sigma^2}\right) n_o\Big(\gamma_v(E-vp_x),T\Big)\;, \quad \text{(A.8)}$$

where here the integration region is $[(m_1,\infty)\times(0,\sqrt{(E^2-m_1^2)})]$.

We need to now integrate over the thickness of the wall. If there are $N\sim\delta/s$ slices, we write

$$F_x = \sum_{n=0}^{N}\Delta P_n\;, \quad \text{(A.9)}$$

where here ΔP_n is the sum of eqs. (A.6)-(A.8) with m_o the mass at the $n^{\rm th}$ step, given by

$$m_o^2 = \int_{+\infty}^{x_n} dx\frac{dm^2}{d\phi}\frac{d\phi}{dx}\sim m^2\frac{n^2}{N^2}\;, \quad \text{(A.10)}$$

In the last step we have made a linear approximation to the wall profile.

We may proceed in a variety of ways. If we assume that the speed of the wall is small, we can expand the distribution (A.4) to lowest order in v. On the other hand, we could expand in powers of m/T, at the risk of making a small error for the top quark. In this Appendix, we will choose the former expansion. We find

$$n_o\Big(\gamma_v(E-vp_x)\Big) = n_o(E) - vp_x\,\frac{\partial n_o}{\partial E}(E) + O(v^2)\;. \quad \text{(A.11)}$$

To lowest order we have:

$$\begin{aligned}\Delta P_n^{[0]} &= \frac{2}{3}\int_{m_o}^{\infty}\frac{dE}{4\pi^2}\; n_o(E,T)\,(E^2-m_o^2)^{3/2} - (m_o\leftrightarrow m_1)\\ &= F(m_o,T)-F(m_1,T)\;. \quad \text{(A.12)}\end{aligned}$$

Summing over the wall and over species, we find the simple result

$$F_x^{[0]} = F(0)-F(m^2)\;. \quad \text{(A.13)}$$

The pressure difference, to lowest order, is the difference of free energy densities. We have neglected contributions proportional to gradients in temperature and chemical potential.

The next-to-leading order terms account for the forces of the plasma on the wall. To order v^1, we find

$$\begin{aligned}\Delta P_n^{[1]} &= -2v\int_{m_0}^{m_1}\frac{dE}{4\pi^2}\,n_o(E)\,E(E^2-m_o^2) \\ &\quad -v\int_{m_1}^{\infty}\frac{dE}{4\pi^2}\,n_o(E)\,E\left(\sqrt{(E^2-m_1^2)}-\sqrt{(E^2-m_o^2)}\right)^2 .\end{aligned} \tag{A.14}$$

The next step is to sum this over the wall. We will do this for the three cases separately. For the thin wall, we simply take $N=1$, $m_o=0$ and $m_1=m$, and obtain

$$F_x^{[1]} = v\left(\rho(0)-\rho(m)-m^2\int_m^{\infty}\frac{dE}{4\pi^2}En_o(E)\right) = v\mathcal{E}\ . \tag{A.15}$$

It is useful to expand this expression in powers of m/T. For W and Z bosons, we find

$$\mathcal{E}_b^{thin} \simeq \frac{3}{\pi}ET\phi^3+\frac{3\phi^4}{64\pi^2v_o^4}\left[2m_W^4\left(\ln\frac{m_W^2\phi^2}{a_Bv_o^2T^2}-\frac{7}{2}\right)+m_Z^4\left(\ln\frac{m_Z^2\phi^2}{a_Bv_o^2T^2}-\frac{7}{2}\right)\right] . \tag{A.16}$$

Likewise, for top quarks, we find[14]

$$\mathcal{E}_f^{thin} \simeq -\frac{3\phi^4}{16\pi^2v_o^4}m_t^4\left[\ln\frac{m_t^2\phi^2}{a_Fv_o^2T^2}-\frac{7}{2}\right]+O((\frac{m}{T})^5) \tag{A.17}$$

The total $\mathcal{E}$ is then

$$\mathcal{E} \simeq \frac{3}{\pi}ET\phi^3+\frac{1}{4}\phi^4\left[\lambda-\lambda_T+2B\left(4\ln\frac{\phi}{v_o}-7\right)\right] . \tag{A.18}$$

If the wall is much thicker than any relevant mean free path, we take s proportional to dx. We can easily see that (A.14) has no linear term in dx,

[14]The expansion is less trustworthy here; in particular, we have neglected terms of order $(\frac{m}{T})^5$.

and we recover Turok's result [30] that there is no v-dependence in the force on the wall in the limit $\ell \to 0$.[15] Presumably there are other effects that are ignored in this computation that slow down the wall.

The case of greatest interest is finite ℓ/δ. We have performed the analysis numerically and find $\mathcal{E}$ is suppressed essentially by a factor of $(\ell/\delta)^{1/2}$. (This non-analytic behavior is expected of eq. (A.14), since its Taylor expansion has singularities at order σ^4.) We can now write $\mathcal{E}$ in the following form:

$$\mathcal{E} = \mathcal{S}_f \mathcal{E}_f^{thin} + \mathcal{S}_b \mathcal{E}_b^{thin} \ . \tag{A.19}$$

where

$$\mathcal{S}_i = \frac{\mathcal{E}_i}{\mathcal{E}_i^{thin}} \ . \tag{A.20}$$

$\mathcal{S}_f$ and $\mathcal{S}_b$ are rather insensitive to m_t and m_H. We have plotted these factors in Fig. 9 *vs.* $(\ell/\delta)^{1/2}$. The behavior of this plot is adequately approximated by a linear function:

$$\mathcal{S}_i \sim \left(\frac{\ell}{\delta}\right)^{1/2} \tag{A.21}$$

for both fermions and bosons. We find then, that the wall velocity, for $m_H = 35$ GeV and $m_t = 120$ GeV, is approximately $v \sim 0.2$ (see Fig. 10).

[15] We have explicitly checked this through order v^2.

References

[1] D.A. Kirzhnits, JETP Lett. **15** (1972) 529; D.A. Kirzhnits and A.D. Linde, Phys. Lett. **72B** (1972) 471.

[2] S. Weinberg, Phys. Rev. **D9** (1974) 3357; L. Dolan and R. Jackiw, Phys. Rev. **D9** (1974) 3320; D.A. Kirzhnits and A.D. Linde, JETP **40** (1974) 628.

[3] D.A. Kirzhnits and A.D. Linde, Ann. Phys. **101** (1976) 195.

[4] A.D. Linde, Phys.Lett. **99B** (1981) 391.

[5] A.D. Linde, Rep. Prog. Phys. **42** (1979) 389.

[6] A.H. Guth, Phys. Rev. **D23** (1981) 347;
A.D. Linde, Phys. Lett. **108B** (1982); **114B** (1982) 431; **116B** (1982) 335, 340;
A. Albrecht and P.J. Steinhardt, Phys. Rev. Lett. **48** (1982) 1220.

[7] A.D. Linde, *Particle Physics and Inflationary Cosmology* (Harwood, New York, 1990).

[8] A.D. Linde, Phys.Lett. **70B** (1977) 306.

[9] S. Dimopoulos and L. Susskind, Phys. Rev. **D18** (1978) 4500.

[10] V.A. Kuzmin, V.A. Rubakov and M.E. Shaposhnikov, Phys. Lett. **B155** (1985) 36.

[11] M.E. Shaposhnikov, JETP Lett. **44** (1986) 465; Nucl. Phys. **B287** (1987) 757; Nucl. Phys. **B299** (1988) 797; A.I. Bochkarev, S.Yu. Khlebnikov and M.E. Shaposhnikov, Nucl. Phys. **B329** (1990) 490.

[12] L. McLerran, Phys. Rev. Lett. **62** (1989) 1075.

[13] L. McLerran, M. Shaposhnikov, N. Turok and M. Voloshin, Phys. Lett. **256B** (1991) 451.

[14] N. Turok and P. Zadrozny, Phys. Rev. Lett. **65** (1990) 2331; Nucl. Phys. **B358** (1991) 471.

[15] M. Dine, P. Huet, R. Singleton and L. Susskind, Phys.Lett. **257B** (1991) 351.

[16] A. Cohen, D.B. Kaplan and A.E. Nelson, Nucl. Phys. **B349** (1991) 727.

[17] A. Cohen, D.B. Kaplan and A.E. Nelson, Phys.Lett. **263B** (1991) 86.

[18] A. Cohen, D.B. Kaplan and A.E. Nelson, University of California, San Diego, preprint UCSD-PTH-91-20 (1991)

[19] A. Bochkarev, S. Kuzmin and M. Shaposhnikov, Phys. Lett. **244B** (1990) 27.

[20] ALEPH, DELPHI, L3 and OPAL Collaborations, as presented by M. Davier, Proceedings of the International Lepton-Photon Symposium and Europhysics Conference on High Energy Physics, eds. S. Hegerty, K. Potter and E. Quercigh (Geneva, 1991), to appear.

[21] M. Dine, P. Huet and R. Singleton, University of California, Santa Cruz, preprint SCIPP 91/08 (1991); A.D. Linde and D.A. Linde, unpublished.

[22] G. Anderson and L. Hall, LBL preprint LBL-31169 (1991).

[23] D. Brahm and S. Hsu, Caltech preprints CALT-68-1705 and CALT-68-1762 (1991).

[24] M.E. Shaposhnikov, CERN preprint TH.6319/91 (1991).

[25] M. Dine, R. Leigh, P. Huet, A. Linde and D. Linde, preprint SCIPP-92-06, SLAC-Pub-5740, SU-ITP-92-6 (1992).

[26] M.E. Carrington, Minnesota preprint TPI-MINN-91/48-T.

[27] A.D. Linde, Phys.Lett. **70B** (1977) 306; **100B** (1981) 37; Nucl. Phys. **B216** (1983) 421.

[28] M. Gleiser and E. Kolb, FNAL preprint FERMILAB-Pub-91/305-A (1991).

[29] N. Tetradis, preprint DESY 91-151.

[30] N. Turok, Princeton preprint PUPT-91-1273.

[31] M. Sher, Phys. Rep. **179** (1989) 273.

[32] J.I. Kapusta, *Finite Temperature Field Theory*, Cambridge University Press, 1989.

[33] V.V. Klimov, Sov. Phys. JETP **55** (1982) 199; G. Gatoff and J. Kapusta, Phys. Rev. **D41** (1990) 611.

[34] S. Coleman, Phys. Rev. **D15** (1977) 2929.

[35] A.D. Linde, Phys. Lett. **93B** (1980) 327;
D.J. Gross, R.D. Pisarski and L.G. Yaffe, Rev. Mod. Phys. **53** (1981) 1.

[36] M. Gleiser, E. Kolb and R. Watkins, Nucl. Phys. **B364** (1991) 411.

[37] A.D. Linde, Stanford University preprint SU-ITP-900 (1991), to be published in Nucl. Phys.

[38] A.M. Srivastava, University of Minnesota preprints TPI-MINN-91/23-T and TPI-MINN-91/37-T (1991).

[39] E. Braaten and M.H. Thoma, LBL preprint LBL-30998 (1991).

[40] E.V. Shuryak, JETP **47** (1978) 212; O.K. Kalashnikov and V.V. Klimov, Sov. J. Nucl. Phys. **31** (1980) 699; H.A. Weldon, Phys. Rev. **D26** (1982) 1384, 2789; E. Braaten and R. Pisarski, Phys. Rev. **D42** (1990) 2156.

Figure Captions

1. The potential $V(\phi, T)$ at the critical temperature T_c and the tunneling temperature T_t, using the (unimproved) one-loop result.
2. The shape of the critical bubble at T_c.
3. The function $f(\alpha)$ describing tunneling amplitude.
4. One-loop tadpole diagrams involving transverse gauge bosons (squiggly line), Coulomb line (dashed), and scalars (solid).
5. The scalar field at the tunneling temperature, T_t, *vs.* m_H.
6. The temperature T_t (plotted as ϵ) *vs.* m_H.
7. The velocity of the bubble wall, v, in the thin wall approximation *vs.* ϵ.
8. The velocity of the bubble wall, v, in the thin wall approximation, *vs.* m_t.
9. The thick wall correction factor $\mathcal{S}$ *vs.* $\sqrt{\ell/\delta}$.
10. The velocity of the bubble wall in the thick wall approximation for specific values of $\mathcal{S}_f$ and $\mathcal{S}_b$.

Fig. 1: Effective Potential

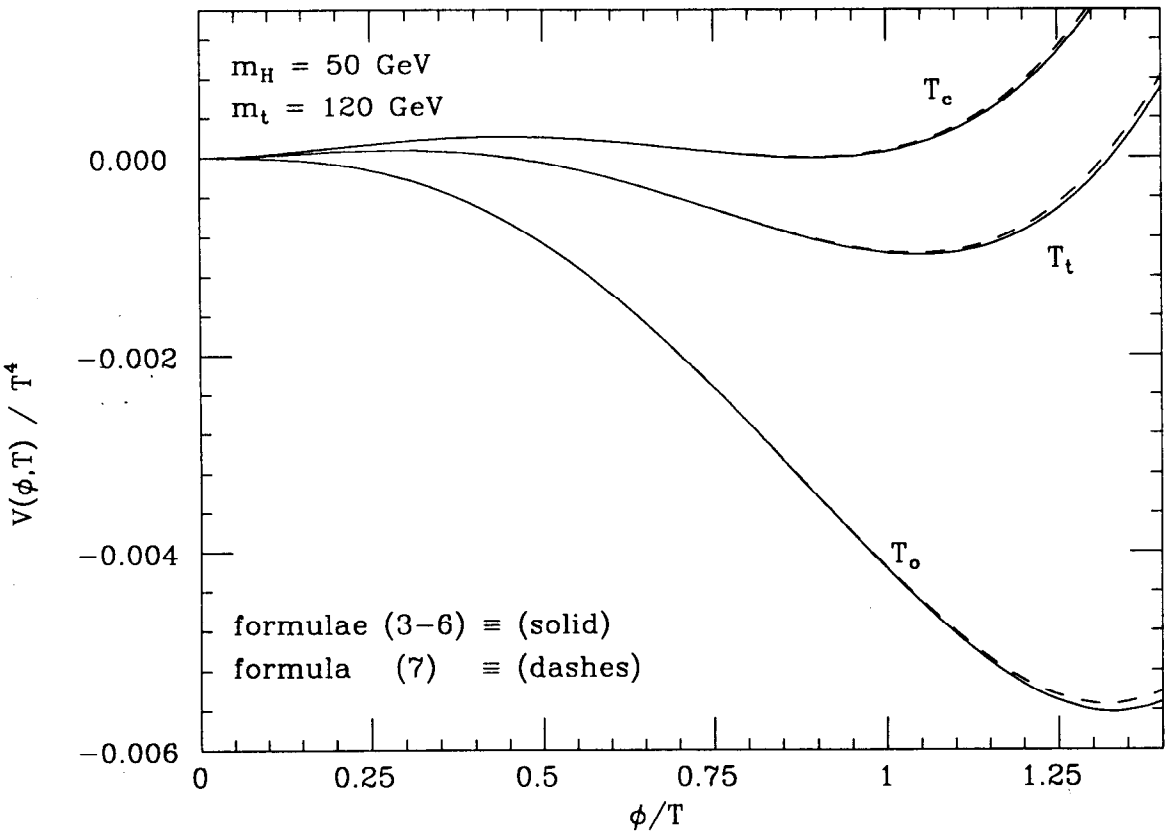

Fig. 2: Shape of the Critical Bubble at T_c

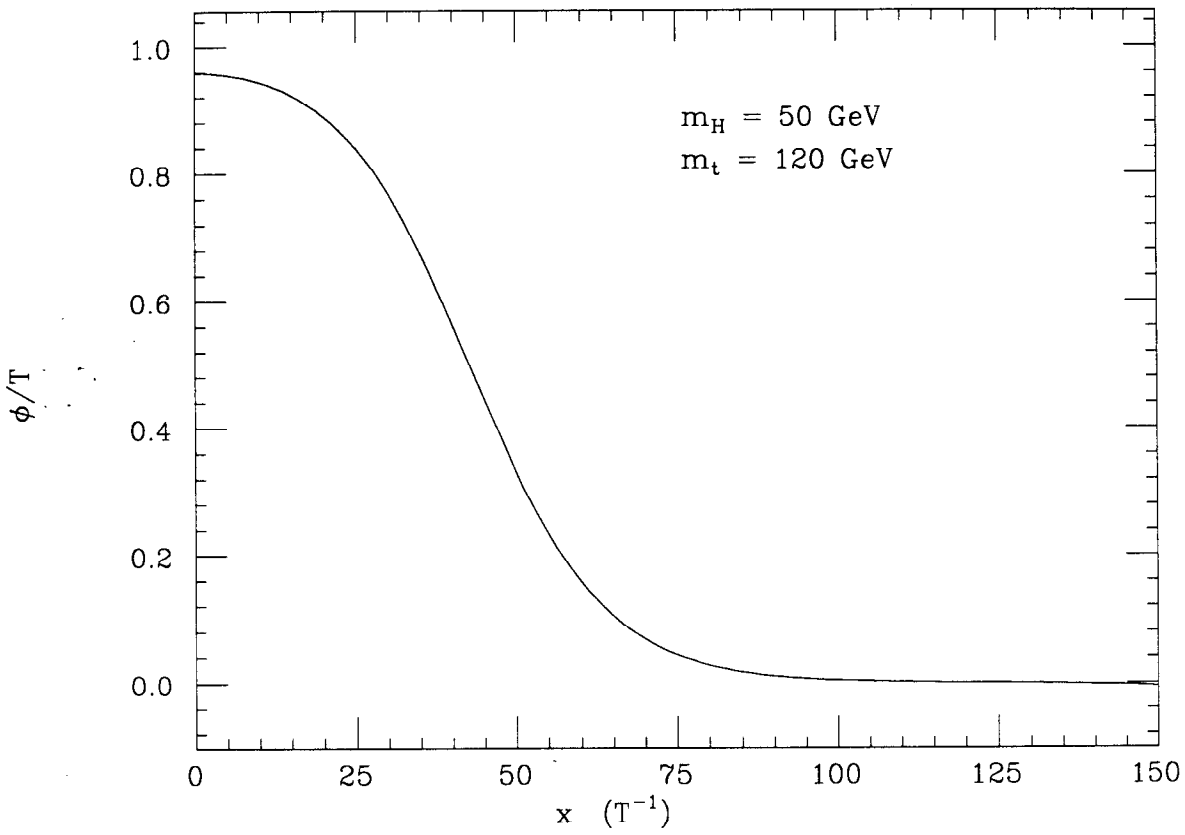

Fig. 3: Tunneling function $f(\alpha)$

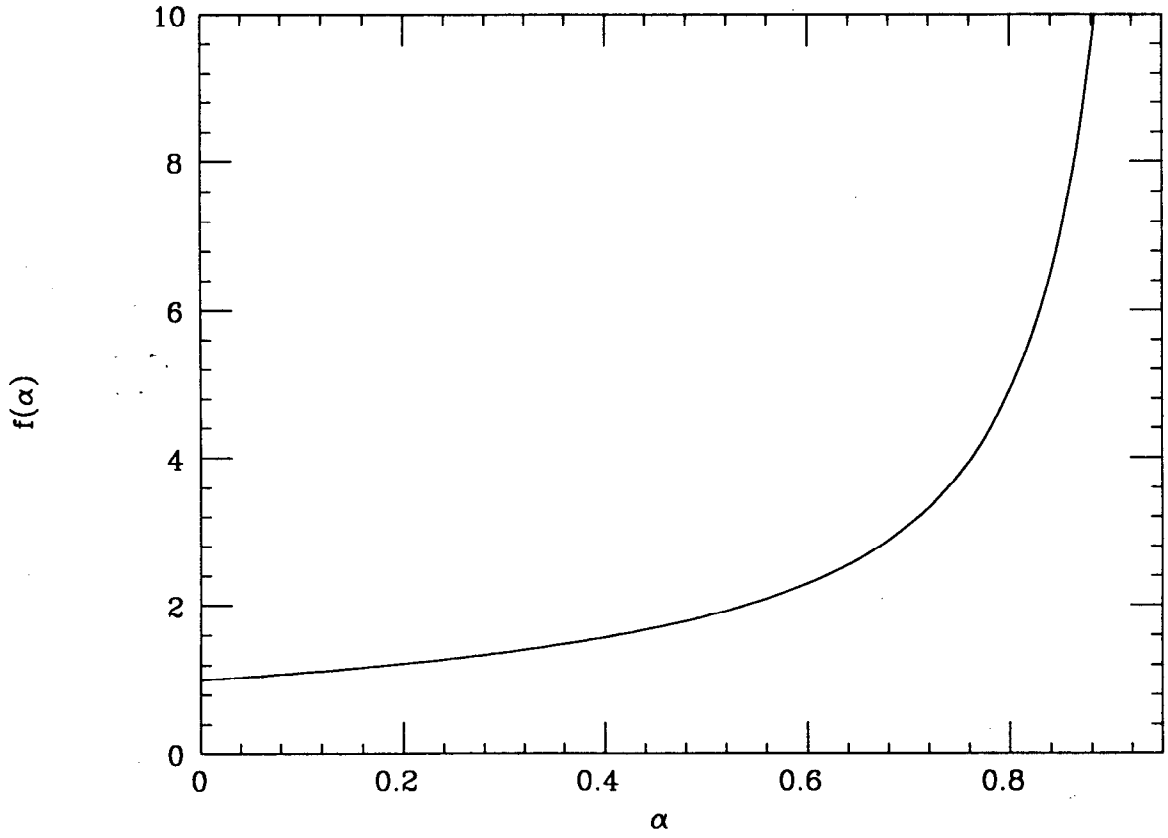

Fig. 4

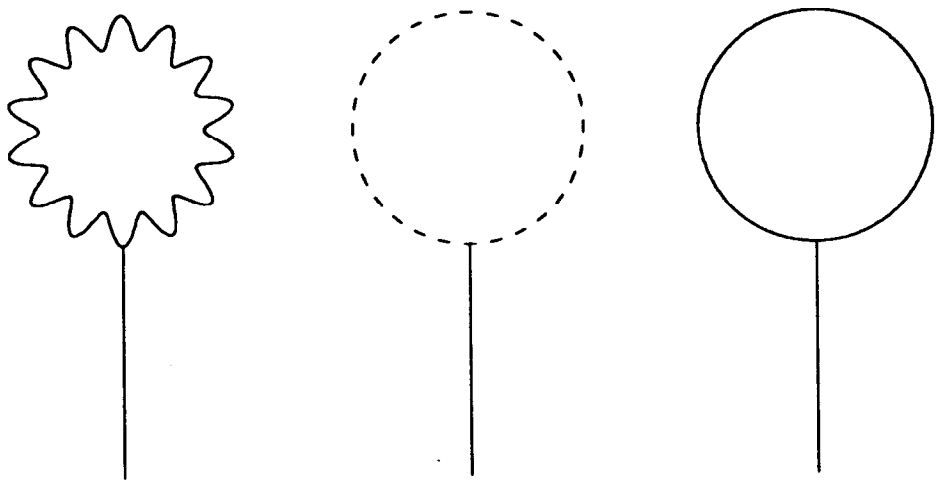

Fig. 5: ϕ/T at T_t

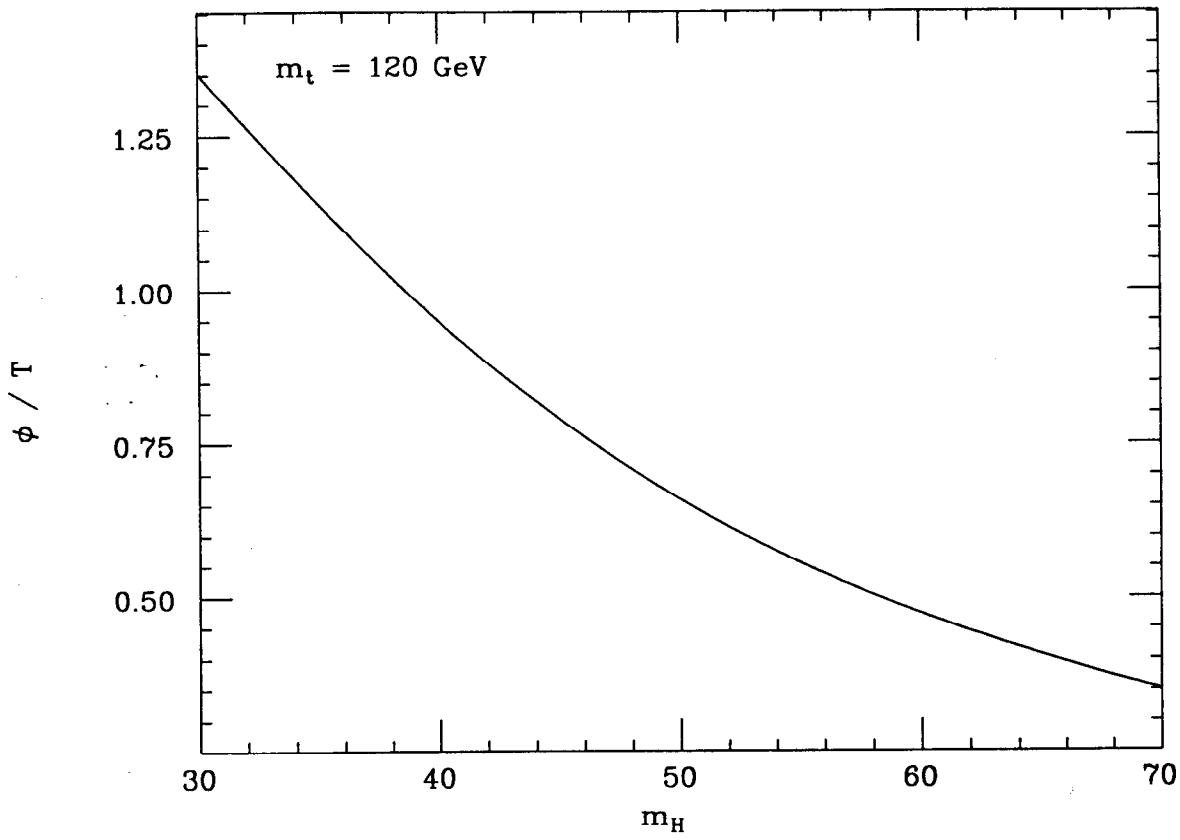

Fig. 6: ϵ vs. m_H

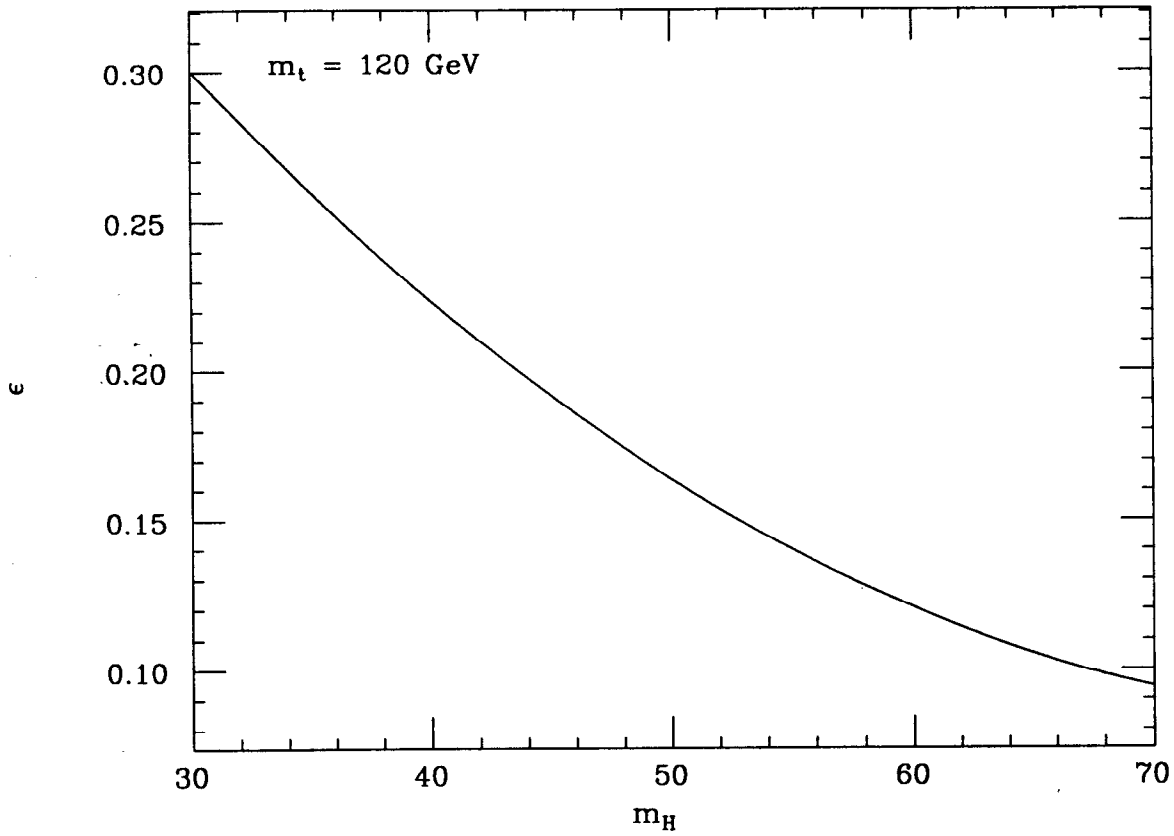

Fig. 7: Wall Velocity vs. Temperature

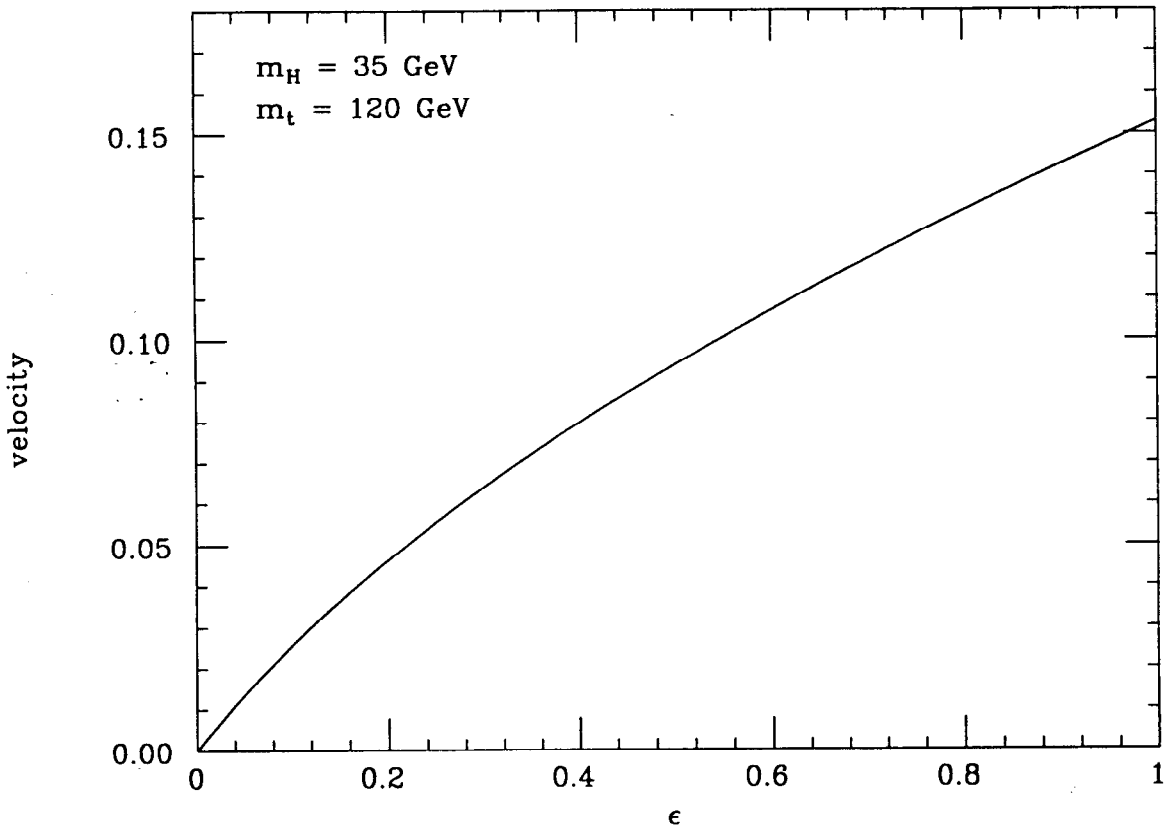

Fig. 8: (Thin Wall) Velocity vs. m_t

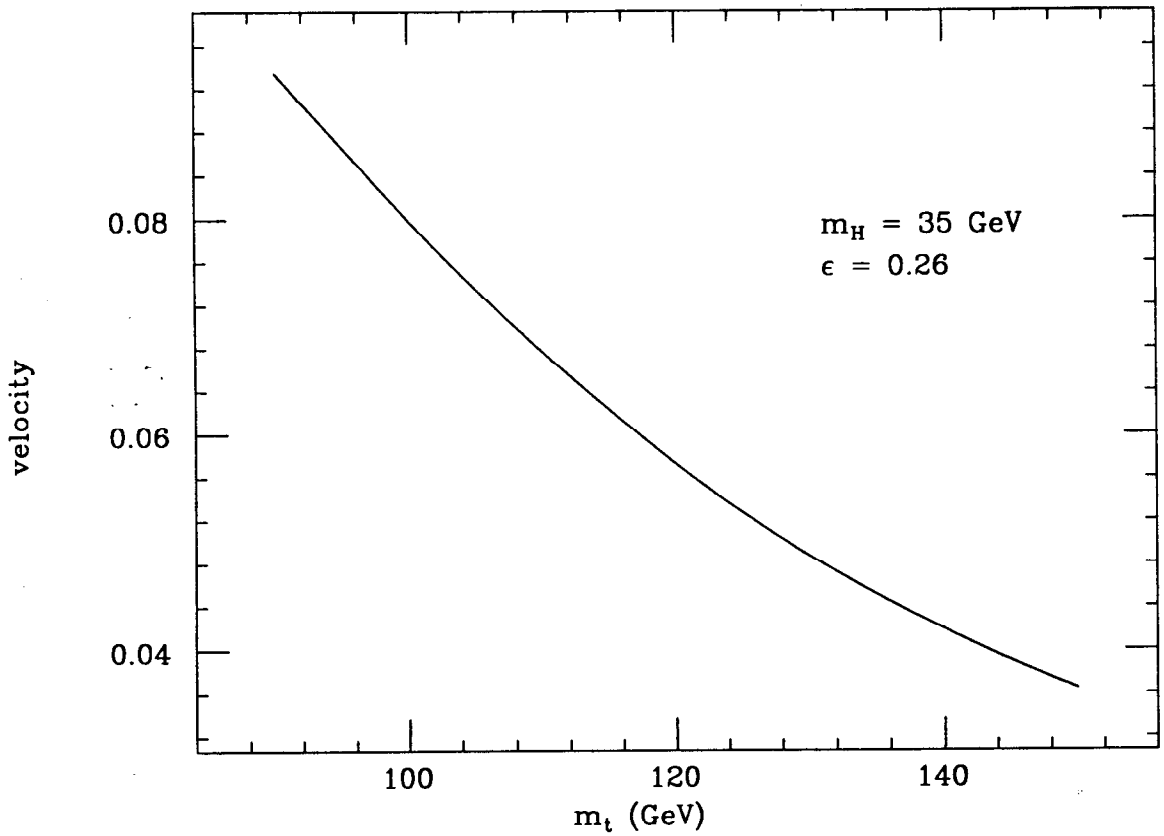

Fig. 9: Suppression Factors S_f and S_b

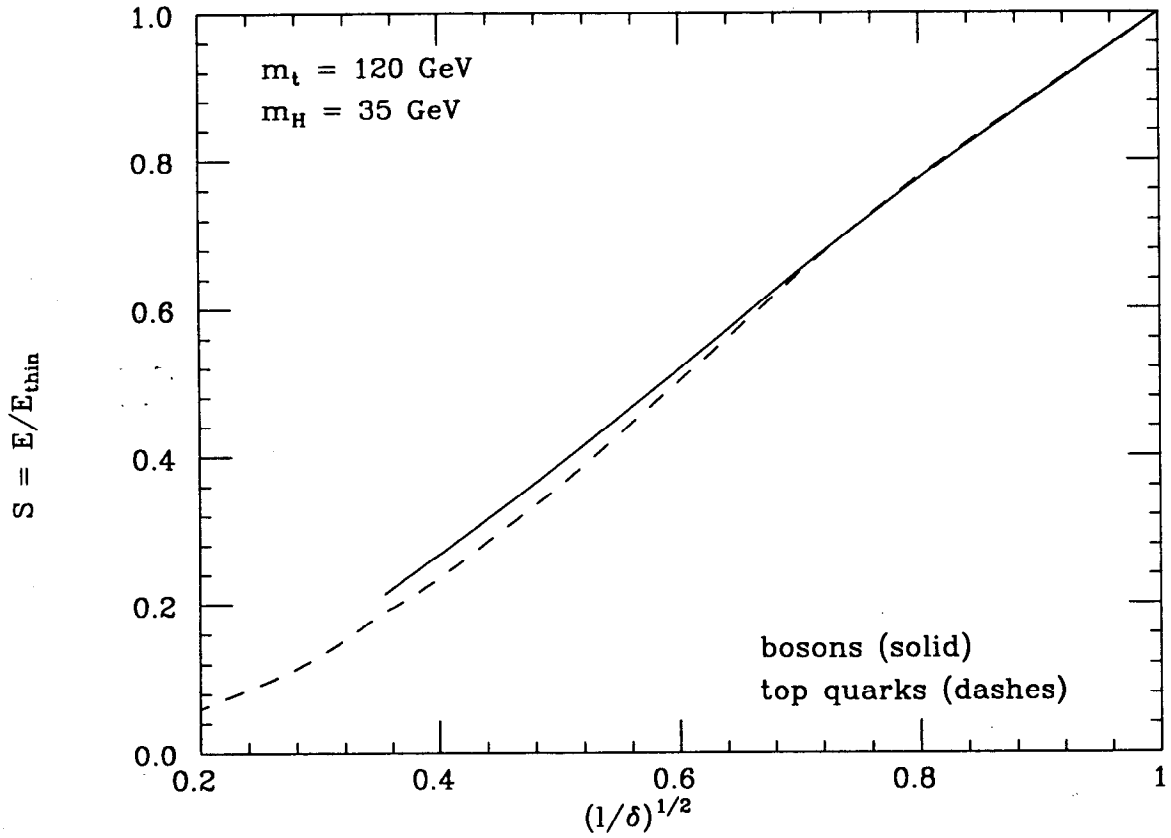

Fig. 10: (Thick Wall) Velocity vs. m_t

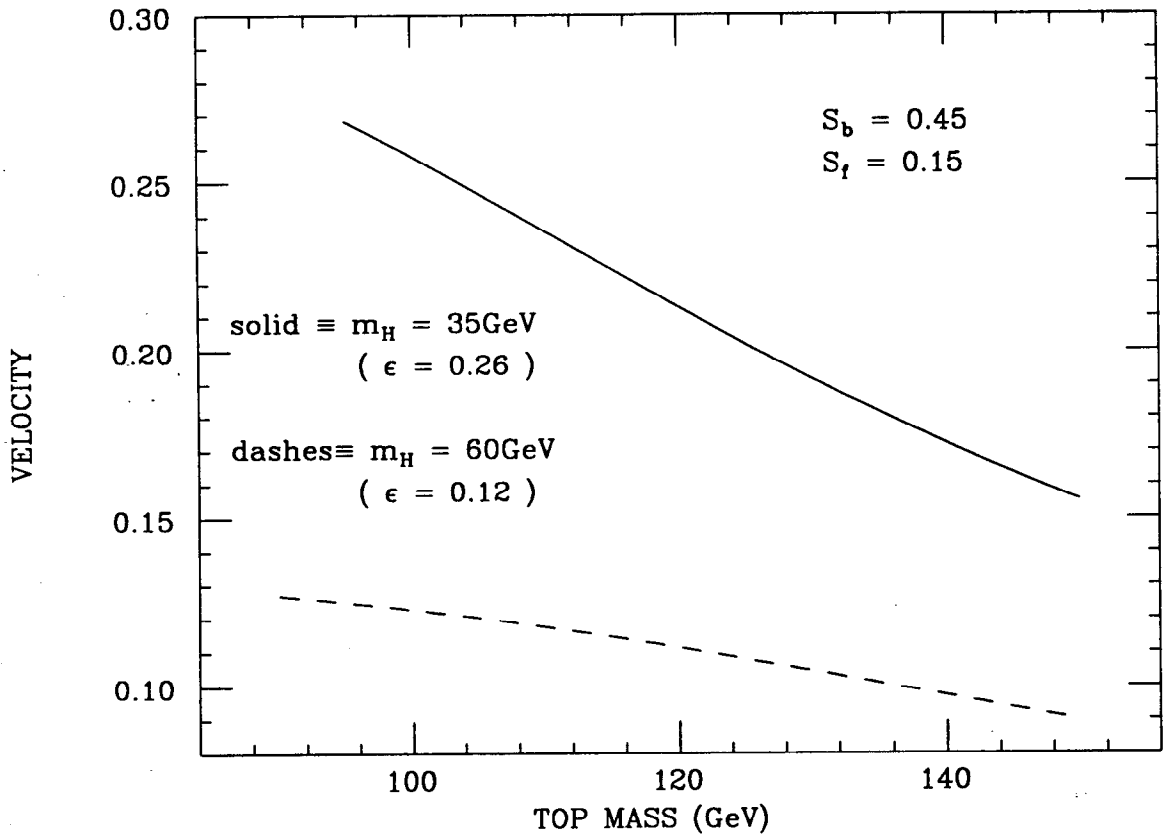

All previous pa-
pers on electroweak phase transi-
tions were wrong, and this one is no bet-
ter. Weak interactions are too weak to produce
strongly first order phase transitions which produce baryons
which produce people which produce papers which explain
why there is something rather than nothing. Bubbles are
formed with thick walls, but as they move, they become thin
since otherwise our approximation does not work. If our
approximation works, top quarks that stick make the wall
very thick, which means that our approximation does not
work anyway. To overcome the controversy, we perform
a detailed study of the flu of quarks at the sick
wall in the high fever approximation. Our
main result is that sick walls drive
quarks crazy.

Fig. 11. Results of computer simulation of the criticall bubble. Apparent inhomogeneity of the bubble is obviously related to the periodic structure of the universe.